2007

Ultrasonic welding of aluminum: a practical study in consistency, part marking and control modes

Maria Vlad
Iowa State University

Ultrasonic welding of aluminum: a practical study in consistency, part marking and control modes

by

Maria Vlad

A dissertation submitted to the graduate faculty

in partial fulfillment of the requirements for the degree of

DOCTOR OF PHILOSOPHY

Major: Industrial and Agricultural Technology

Program of Study Committee:
David Grewell, Major Professor
Ramesh Kanwar
Carl Bern
Michael Kessler
Johannes van Leeuwen

Iowa State University

Ames, Iowa

2007

Dedication

This work is dedicated to my family: my mother, Maria Baboi, my father, Gheorghe Baboi, and my older sisters. Even if they cannot witness my accomplishment, I know they always believed in me and their daily advice was: “Hard work is always paid off!” I wish nothing more than to make them proud of my professional achievements, as they always made me feel proud of them.

TABLE OF CONTENTS

LIST OF TABLES

LIST OF FIGURES

LIST OF SYMBOLS

θ Temperature (°C)

κ Thermal diffusivity (m^2/s)

λ Thermal conductivity (W/(m·°C)

C Specific heat (Joules/(kg·°C)

P Power (W)

q Heat flux (W/m^2)

ω Angular frequency (Rad/s).

F Frictional force (N)

A_0 Amplitude (m)

t Time (s)

x Distance (m)

f Applied normal force (N)

μ Dynamic coefficient of friction

ν Frequency (Hz=1/s)

v Velocity (m/s)

ACKNOWLEDGMENTS

This study was funded by Ford Co. in cooperation with Branson Co. from Danbury, CT. I want to give special thanks to all my colleagues that I have worked with and shared their welding knowledge with me: Jay Sheehan, Jon Wnek, Jon Piasecki, Rich Hansen, Roland Scott.

Special thanks to my committee members: Ramesh Kanwar, Michael Kessler, Johannes van Leeuwen, Carl Bern, David Grewell for accepting to be part of one of my highest achievements in life.

I will always be grateful to my major professor Dr. David Grewell who opened up a new door in my life showing me and proving me that if there is will, everything can be possible. He was and will always be the greatest mentor and instructor I have ever had, by showing me the light of a tunnel that was completely dark before: self confidence. There are no words to thank you enough, Dr. Grewell for everything you have done for me.

ABSTRACT

Patented in 1960, ultrasonic welding for metals, has received significant research and there have been advances in the technology. Because of these advances, the process has been developed into a practical production tool. Although the ultrasonic metal welding has many advantages including speed, efficiency, long tool life, there are several issues. For example, tool/part adhesion (sticking), part marking and the lack of the consistency and predictability of the weld strength are issues that industry currently encounters with ultrasonic metal welding. To resolve these issues of the ultrasonic metal welding process, various experiments have been conducted on aluminum 5754 alloy samples. These experiments included replacing a constant amplitude with amplitude profiling and placing buffer sheets of copper and zinc between the tool (horn) and the top part prior to ultrasonic welding. In addition, experiments were conducted to compare the consistency of weld strength for the three control modes: energy, height (post height), and time. Their results were analyzed and compared in terms of weld strength, weld consistency and weld quality.

It was seen that amplitude profiling produced an increase in weld strength, however the part marking and the tool/part adhesion were not reduced. By matching the amplitude to the various weld phases, the weld cycle was optimized to produce relatively strong welds and weld cycle time was reduced. For example, by initiating the weld cycle with a relatively high amplitude, the asperity peaks are sheared, heating and softening of the faying surfaces are completed quickly and efficiently. Then by reducing the

amplitude at the end of the weld cycle, shearing of the weld is reduced and weld damage is minimized resulting in relatively strong welds.

Very simple models based on frictional heating were able to predict power dissipation reasonably well. When these models were coupled with a one dimensional heat flow solution, the initial bondline temperatures were accurately predicted. However, the predicted temperatures diverged from the measured temperatures as a function of cycle time. It is believed that this deviation was due to the over simplified assumptions used to model the process. For example, the assumption that the process could be modeled with one dimensional heat flow in a semi-infinite body was seen to be false shortly after the weld process was initiated.

The study involving the placement of buffer sheets (copper or zinc) between the tool (horn) and the top part prior to the ultrasonic welding process reduced the tool/part adherence and the part marking. However, it was seen the use of buffer sheets slightly lowered the weld strength and this was especially seen for the thicker (3-mm) parts and copper buffer sheets. It was also seen that zinc buffer sheets did not lower weld strength as much as the use of copper buffer sheets.

Also, it was concluded that the weld strength variance for those welds made with the time mode was smaller than that for the welds made in the height and energy mode.

CHAPTER 1: INTRODUCTION

Ultrasonic energy has been used in a wide variety of applications from very low power medical diagnostics to high intensity processes that change the state of materials. Joining of metals, such as nonferrous metals used in electrical connections, is a useful application of this technology. Commonly used joining techniques, such as, those that involve heating by flame, heated tools, electric current or arcs are able to fuse these materials. However, these processes are time consuming, often labor intensive and usually require cleaning and the addition of filler metals. Despite these issues, industry has become accustomed to the issues. However, ultrasonic welding of nonferrous metals in electrical connections has eliminated most, if not all, of these problems. In fact, ultrasonic welding of metals is becoming a popular process by informed design and manufacturing engineers.

This study explores joining various thicknesses of aluminum alloy 5754 with ultrasonic energy, in order to find the optimum parameters and conditions of this technology. Its final application will be the production of the aluminum automobile frames.

The first chapter of the paper is a general overview of the aluminum, aluminum alloys, the advantages and disadvantages of using aluminum alloys for the cars frames and the benefit of aluminum recycling. Also, this chapter briefly presents other joining methods that are commonly used such as: gas metal arc welding, gas tungsten arc welding, adhesive bonding, followed up by a detailed description of the ultrasonic metal welding equipment and its implications.

Aluminum

Researchers state that, "aluminum comprises 8% of the earth's crust and is, therefore the most abundant structural metal" [1]. Its production is higher than that of copper, and second compared to iron. Initially its unit price was very high which steadily decreased with new smelting technologies. Today the price of aluminum is lower than the price of copper. Because of its electrical properties it is competing with copper in the electric and construction industry. Although the electrical conductivity of aluminum is slightly lower than that of copper, it is preferred over copper in power cables because of its lighter weight. Aluminum used in the industry can be anodized to produce a protective oxide film, which can be dyed to give a colorful appearance. The anodizing process uses a bath of dilute sulfuric acid as an electrolyte and charging the piece electrically. The piece that is being anodized is the anode –the positive pole -- and the electrolyte becomes the negative pole –the cathode. The electrical charge and the mild acid oxidize the aluminum surface, leading to microscopic crystals of aluminum oxide, which is very hard, but very porous. This porosity is responsible for absorbing and holding the colors of the dye. After the anodized part is removed from the bath it is dipped into a container of concentrated color (dye) for several minutes. After dying, the part is immersed in clean, boiling water for several minutes to close the pores and seal the dye by hydrating the crystalline layer and swelling the oxide.

Aluminum alloys

When the electrolytic reduction of alumina (Al_2O_3) (produced from bauxite) was developed by Charles Hall in Ohio and Paul Heroult in France in 1886, the first

“aluminum internal-combustion-engine-powered vehicles” appeared, and aluminum started to play an important role in the automotive industry [2]. Since then, alloys of aluminum have been developed, improving its properties and making it extremely popular in different industries. These alloys are light weight, strong, electrically and thermally conductive and have good corrosion resistance.

Aluminum alloys can be divided into two major categories: casting and wrought. Cast is aluminum produced in a foundry. Aluminum ingots are melted in furnaces and the molten aluminum is poured into molds. Wrought is the aluminum formed of sheet, strip or bar stock that is “hand-worked”. The aluminum is heated in a forge and hammered to shape.

For wrought alloys a four digit system is used to produce a list of wrought composition families as follows [2]:

- 1xxx Controlled unalloyed (pure) composition. Used primarily in the electrical and chemical industries.
- 2xxx Alloys in which copper is the principal alloying element, though other elements, notably magnesium, may be specified. They are widely used in aircraft.
- 3xxx Alloys in which manganese is the principal alloying element. Used as a general purpose alloy for architectural applications and various products.
- 4xxx Alloys in which silicon is the principal alloying element. Used in welding rods and brazing sheet.
- 5xxx Alloys in which magnesium is the principal alloying element. Used in boat hulls and other products exposed to marine environments.

- 6xxx Alloys in which magnesium and silicon are principal alloying elements. Commonly used for architectural extrusions.
- 7xxx Alloys in which zinc is the principal alloying element, but other elements such as copper, magnesium, chromium and zirconium may be specified. Used in aircraft structural components and other high-strength applications.
- 8xxx Alloys including tin and some lithium compositions, characterizing miscellaneous compositions.

Casting compositions are described by a three-digit system followed by a decimal value. The term “heat treatable” for the aluminium alloys, both wrought and cast, is used for specific operations employed to increase strength and hardness by precipitation hardening. Thus the term heat treatable distinguishes these alloys from those alloys in which no significant strength improvement can be achieved by heating and cooling [3].

Cold working

The non-heat treatable alloys depend primarily on cold work to increase mechanical properties. Cold work occurs as a consequence of plastic deformation at low to moderate temperatures. Such deformation increases the concentration of dislocations. Energy is added to the material, being applied fast enough and in large enough magnitude to not only move existing dislocations, but also to produce a high number of new dislocations. A metal filled with dislocations will hinder the movement of any one large dislocation. Thus plastic deformation cannot occur at normal stress levels where work hardening is been completed. That is to say, the small dislocations act as crack inhibitors

which stop large fracture defects from growing. A much higher force is required in order to overcome the strain-field interactions and break the cold worked material. Therefore, the yield strength is increased.

Heat treating

Annealing is a process that produces equilibrium conditions by heating and maintaining at a certain temperature and cooling very slowly to allow the internal stresses to be relieved. Three phases take place during annealing: recovery, re-crystallization and grain growth. In the recovery phase the metal is softened by removal of the crystal defects and internal stresses. Second phase, re-crystallization consists of new grains nucleation and grow, replacing those crystals that have internal stresses. If annealing is allowed to continue beyond the re-crystallization completion, the grains start to grow, leading to a coarsen microstructure (less than satisfactory mechanical properties).

Annealing is applied to both grades of aluminium to promote softening. Complete and partial annealing heat treatments are the only ones used for the non-heat treatable alloys. The exception is the 5000 series alloys which are sometimes given low temperature stabilisation treatment.

Annealing is carried out in the range 300-410°C depending on the alloy. Heating times vary from 0.5 to 3 hours, depending on the size of the load and the alloy type. Rate of cooling after annealing is not critical.

Solution heat treatment is applicable to the heat treatable alloys and involves a heat treatment process by which the alloying constituents are taken into a solution and retained by rapid quenching. Subsequent heat treatment at lower temperatures, such as

ageing or natural ageing at room temperature, allows for a controlled precipitation of the constituents, thus achieving increased hardness and strength.

Time at temperature for solution treatment depends on the type of alloy and the furnace load. Sufficient time must be allowed to take the alloys into solution if optimum properties are to be obtained.

The speed of quenching is important. Generally, rapid formation of precipitates of constituents begins at around 450°C for most alloys and it must not fall below this temperature prior to quenching [3].

The usual quenching medium is water at room temperature, although in some circumstances "slow quenching is desirable, as this improves the resistance to stress corrosion cracking of certain copper-free Al-Zn-Mg alloys" [3].

Parts with complex shapes may be quenched at slower quenching rates to decrease distortion.

After solution treatment and quenching, hardening is achieved either at room temperature (natural ageing) or with a precipitation heat treatment (artificial ageing). In some alloys sufficient precipitation occurs in a few days at room temperature to yield stable products with the desired properties. However, in some cases these alloys are precipitation heat treated to provide increased strength and hardness in wrought and cast alloys. Other alloys with slow precipitation reactions at room temperature are heat treated at high temperatures before being used.

Where natural ageing is carried out, the time may vary from around 5 days for the 2xxx series alloys to around 30 days for other alloys. The 6xxx and 7xxx series alloys are considerably less stable at room temperature and continue to exhibit changes in

mechanical properties for many years. With some alloys, natural ageing may be suppressed or delayed for several days by refrigeration at -18°C or lower.

The artificial ageing or precipitation heat treatments are low temperature, long time processes. Temperatures range from 115-200°C and times from 5-48 hours. Accurate temperature control and variation temperatures are critical to the process and generally temperatures should be held to a range of ±7°C.

In order to prevent a significant loss of mechanical properties, the over aging must be avoided. Over aging, consisting of longer times and higher temperatures, leads to larger particles and precipitates. The objective is to select the cycle that produces the optimum precipitate size and distribution pattern. Unfortunately, one cycle may achieve a maximum in one property, such as strength, but it may not provide optimum values for the other properties such as yield strength and corrosion resistance. Consequently, the cycles used represent compromises that provide the best combination of properties.

Automotive applications

Although the use of aluminum in cars has been increasing for the past two decades, progress has been limited in developing aluminum auto bodies. In fact, most aluminum substitutions are castings and forgings in the transmission and wheels. However, aluminum has not been commonly used for auto body panels. The substitution of aluminum for steel in the automobile industry is influenced by different factors such as: fuel efficiency standards, vehicle weight and recycling standards. One of the key obstacles is the slightly higher cost of aluminum (1.52 $/lb) compared to steel (0.38 $/lb) (the calculations are based on blank weight) [16].

Aluminum is a key material for reducing weight without sacrificing safety, comfort and reliability. Because of its low density (1/3 that of steel) and its relatively high strength, its extensive use "can result in up to 300 kg weight reduction in a medium size vehicle (1400 kg), which represents a weight saving of more than 20% of the total car" [5].

Aluminum can be recycled numerous times without loss of quality. Statistics say that "95% of aluminum in cars is collected and recycled and accounts for over 50% of the material value of a vehicle at the end of its life" [5]. Weight reduction ranks high on the priority list of the automotive industry, offering benefits to the consumer and to society as a whole. European researchers state that "reducing the weight of a vehicle by 100 kg allows savings of 0.6 litters/100 km" [5].

The average aluminum content in European automobiles is approximately 65 kg and is continuously growing by 4% annually. In Scandinavia, one of Volvo's largest models contains 140 kg of aluminum. In Germany, Audi launched its "all-aluminum" car, the A8 in 1994. The aluminum used in the Audi A8 model resulted in a 40% reduction in the weight of the car body. Audi pointed out that the additional amount of energy required to produce the body cars from aluminum could be recovered through fuel savings after 60,000 km. "When such a body is produced from 70% recycled metal, aluminum shows an energy advantage from the very first kilometer" [5].

Thus, the use of aluminum in automobiles can reduce energy consumption and pollution.

Recycling

In order to accept aluminum as the "material of the future for automotive applications", its recyclability should be carefully analyzed. Because of the slightly higher value of aluminum relative to other automotive materials, the automotive market recycles aluminum more compared to other industries (higher than aluminum cans, being recycled at a rate of 60%). The majority of aluminum in cars is in the form of castings, therefore the recycled material can be returned to foundries for production of new castings. Researchers state that "projections for both the aluminum used in automobiles and the demand for secondary metal for automotive castings indicate that castings can continue to absorb the aluminum automotive scrap generated in the near term" [6]. However, the wrought products in aluminum body structures are more commonly being recycled back into sheet and extrusion products. There is a large interest in recycling the aluminum from the automobile industry from 85% to 100%, being addressed by "R&D efforts in the area of scrap sorting supported by the Department of Energy's Office of Industrial Technologies and Office of Transportation Technologies in concert with the Aluminum Automotive Alliance organized through The Aluminum Association" [6].

In order to gain insight into recycling process, an overview of the existent infrastructure should be considered. In general, from the consumer the cars are transported to the automotive dismantler to be dismantled for useable parts and easily sorted for high value aluminum components such as wheels and radiators. The remaining components are shredded into relatively small pieces of various materials. Ferrous and non-metallic scrap is separated from the non-ferrous scrap and sent to separators to

remove non-aluminum scrap, such as copper and zinc. The mixed aluminum scrap is sold to the secondary industry for recycling into foundry alloys [6].

It is easy to appreciate the need of recycling aluminum by considering the next 10-15 years, when the current vehicles with much higher overall aluminum content are at the end of their useful lives. Cost-effective methods for the separation of wrought scrap will be needed, to ensure an efficient recycling. This need will grow with the continuous usage of aluminum vehicles utilizing high proportions of wrought products.

Since the recycling of automotive aluminum plays an important role in energy efficiency and environmental conservation, the Department of Energy's Office of Industrial Technologies and Office of Transportation Technologies have funded the development of new sorting and recycling technologies. For example laser-induced breakdown spectroscopy is used for separation of wrought from cast aluminum alloys. Selective etching plus color sorting separates the wrought alloys into different composition groups [6].

The selective etching plus color sorting technique consists of a caustic etch treatment of the shredded pieces. Since different aluminum alloys react differently to the etch treatment based on their alloying constituents, they can be sorted by the resulting colors. Alcoa has patented a process that enables separation of alloys into three distinct categories: "bright", consisting of pure Al and binary Al-Mg alloys; "gray", consisting of Al-Mg, Al-Si, and Al-Mg-Si alloys; and "dark", consisting of alloys containing Zn and Cu. After the etching, a camera performs the sorting function.

The laser-induced breakdown spectroscopy (LIBS) technique is “an adaptation of the optical emission spectroscopy chemical analysis technique utilized currently for

aluminum alloys" [6]. A laser vaporizes a small region of the sample for analysis instead of a DC arc (as in the conventional method), increasing the processing rate. The spectrum of each sample is analyzed and its chemical composition determined, allowing a "piece-by-piece alloy identification" [6]. According to the reports, up to 50 shredded pieces per second can be analyzed by using the laser-induced breakdown spectroscopy. This technique requires a surface free of paint and protective coatings in order to be effective [6].

Welding of Al

Aluminum has several chemical and physical properties that need to be understood prior to considering various joining processes. While there are alternative techniques to joining aluminum, such as mechanical fasteners and adhesive bonding, only welding is considered in this work. The specific properties that affect welding are its oxide characteristics, the solubility of hydrogen in molten aluminum, its thermal characteristics and its wide range of mechanical properties and melting temperatures that result from alloying [2].

Aluminum has a strong chemical affinity for oxygen and will oxidize rapidly upon exposure in the air. The oxide should be reduced chemically or removed prior to welding. However as will be further detailed, the natural oxide can be removed by ultrasonic welding. The melting temperature of the aluminum oxide is very high (2050^0C), compared to the melting point of the base alloy. If the oxide is not removed, the result is incomplete fusion.

Hydrogen dissolves very rapidly in molten aluminum, being the primary cause of porosity in aluminum welds. The hydrogen is absorbed by the weld pool and, as the pool solidifies, the solubility of hydrogen is greatly reduced, forming gas porosity. However, it has no solubility in solid aluminum, which is the case in the ultrasonic welding. That is to say, ultrasonic welding of aluminum occurs in the solid state and thus, hydrogen solubility is generally not an issue.

Because of the high thermal conductivity of aluminum, energy requirements or power density requirements are critical. Thermal conductivity is "the quantity of heat transmitted through a unit thickness in a direction normal to a surface of unit area, due to a unit temperature gradient under steady state conditions" [15].

The specific heat capacity is the amount of heat required to change a unit mass of a substance by one degree in temperature [15].

The thermal diffusivity is the ratio of thermal conductivity to volumetric heat capacity (density times specific heat capacity).

A comparison between the aluminum and steel thermal conductivity, specific heat, and diffusivity is shown in Table 1 [14, 15].

Table 1: Comparison between aluminum and steel thermal properties

Material Property	Aluminum	Steel
Thermal Conductivity (W/m K)	237	51.9
Specific Heat (kJ/kg K)	0.91	0.49
Thermal Diffusivity (m^2/s)	9.8×10^{-5}	1.65×10^{-5}

As detailed in the table, aluminum has higher thermal properties compared to steel, which suggests that higher steady heat inputs are required when welding aluminum.

The primary methods used in welding aluminum and its alloys are the gas-shielded arc welding processes. Other methods include: resistance welding, friction welding, stud welding and laser-beam and electron-beam welding [2]. Each of these processes is detailed below.

The GTAW (gas-tungsten arc welding) is a process used to weld thicknesses from 0.25 to 150 mm (0.010 to 6 in.) and can be used in all weld positions. It is relatively slow, being used for welding tubing, piping, and variable shapes. It has an excellent penetration control and can produce good welds. Defects, such as weld termination craters, can be filled by reducing the current which is typically controlled with a foot pedal.

Manual gas tungsten arc welding is often considered the most difficult of all the welding processes commonly used in industry. Because the welder must maintain a short arc length, great care and skill are required to prevent contact between the electrode and the work piece. Unlike other welding processes, GTAW normally requires two hands; one hand feeds a filler metal into the weld area while the other manipulates the welding torch. However, some welds combining thin materials (known as autogenous where no

filler rod is used) can be accomplished without filler metal, such as edge, corner and butt joints [7].

The main disadvantage of GTAW is that it produces the slowest metal deposition rate of all the processes. The emphasis is on making welds that are perfect in appearance, which means lower welding current and more welding time are required. The operator needs to learn to coordinate precise movements of the torch in one hand with adding filler metal from the other hand and controlling current with a foot pedal.

GMAW (gas metal arc welding) is a high speed production process for arc welding aluminum. It uses positive electrode dc power and concentrates the arc to produce rapid melting. The aluminum wire is automatically fed through the welding gun, melted at the arc, and then sprayed across the arc. Because the electrode and filler are the same, the process is easily mechanized or adapted for robotic operations [2].

The equipment for GMAW is more complex, more costly and traditionally less portable. Welding is typically done "within a 10 to 12 foot radius of the wire feeder and the work is usually brought to the weld station" [7].

Both non-heat-treatable and heat treatable aluminum alloys can be resistance welded. Resistance spot and seam welding of aluminum alloys are used in manufacturing of cooking utensils, tanks, bridge flooring plus many aircraft and automotive components. Resistance welding of aluminum aircraft components, such as wing-skin sections or deck sections, provides high quality welds, but requires expensive equipment for cleaning, welding and controlling weld quality.

Adhesive bonding is a method by which materials can be joined to generate assemblies. Adhesive bonding is an alternative to more traditional mechanical methods of

joining materials such as: nails, rivets and screws. “An assembly made by the use of an adhesive is called an adhesive joint or an adhesive bond” [8]. Solid materials that need to be bonded are known as the adherents. The process allowing the adhesive to transfer a load from the adherend to the adhesive joint is called adhesion. In general, adhesives are polymeric materials that exhibit viscoelastic properties. Polymer-based adhesives absorb mechanical energy applied to the joint and dissipate that energy as heat. Typically, the fatigue failure of adhesive bonds is longer in comparison with mechanical fastening. One disadvantage of adhesive bonding is its reliance on adhesion for the transfer of load through the assembly. Adhesion is a surface physico-chemical phenomenon. Since adhesion is a surface phenomenon, the physical properties of the adhesive joint depend strongly on the character of the surface of the adherend and how the adhesive interacts with that surface. Thus, an adherend with an “improper surface could lead to lower joint strengths than might be predicted from the mechanical properties of the adhesive and the adherend” [8].

Ultrasonic metal welding (USMW), invented over 50 years ago, is a process that consists of joining two metals by applying ultrasonic vibrations under moderate pressure. The high frequency vibrations locally soften the overlap zone between the parts to be welded forming a solid-state weld through progressive shearing and plastic deformation. The oxides and contaminants are removed by the high frequency motion (“scrubbing”) producing a pure metal/metal contact between the parts which allow the intermetallic bonding to take place. Researchers state that “Ultrasonic welding of metals consist of interrelated, complex processes such as plastic deformation, work hardening, breaking of contaminant films, fatigue crack formation and propagation, fracture, generation of heat

by friction and plastic deformation, re-crystallization, and interdiffusion." Also, it is worth noting that "the dominating mechanism for ultrasonic welding is solid state bonding, and it is accomplished by two different processes: Slip and plastic deformation."

A key attractive feature of USMW is that it is a solid-state bonding process, so issues involving melting, resolidification of the base metals, with the resulting impact on material properties, do not occur. It is important however, to note that heat affected zone may experience morphological changes because of the heating.

Beyer [10] studied diffusion in ultrasonic welding for long periods of time with copper and aluminum. Temperatures close to or slightly higher than the melting point of the materials to be welded were found at the faying surfaces which explained the diffusion bonding. However, the metallurgical examination did not show any evidence of melting. Also, Beyer found that immediately after the ultrasound was applied, micro-joints at the weld interface were formed. Hazlett's et al [11] research studied the diffusion phenomenon and determined that bonding occurs along the grain boundaries rather then in the bulk of the material.

There is a significant difference between welding metals of plates and welding wire or sheets. Pflueger et al. [12] shares Hazlett's opinion [11] that "in wire bonding there is no gross interface sliding but a great deal of external plastic deformation". The process that takes place during welding of sheets is dependent on the internal deformation of the sheet which allows the interface to slide. In welding a wire to a substrate, the wire does not move relative to the substrate, which results in less internal deformation of the substrate. Therefore there is less heat generation at the interface and the wire is squeezed onto the substrate with significant deformation in the wire only. Wire bonding was a

topic described in detail by Joshi [9]. His results were significantly different from the majority of the results on the sheet metal welding (i.e. no sliding, no heating).

Equipment

The principal set-up for ultrasonic metal welding is shown in Figure 1. In a typical weld the joining of the overlapping sheets will occur in the deformation zone at the part interface directly beneath the horn.

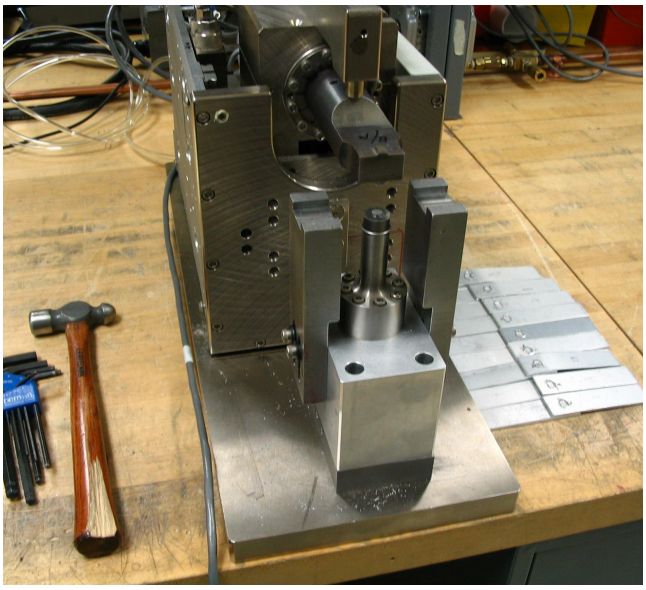

Figure 1 Ultrasonic metal welding equipment

The system components (Figure 2) are: the transducer (converter), a booster with a mounting ring and a horn. It is important to note that in nearly all commercial systems, the systems are designed to resonate at a particular frequency to maximize the overall efficiency. The selection of the frequency is detailed in the following paragraph.

The power supply/generator converts commonly available line voltage electrical power into high frequency electrical energy. Although any frequency between 15 kHz and 70 kHz could be used, 20 kHz is the most popular.

The converter changes the electrical energy into low-amplitude mechanical vibrations of the same frequency.

The booster couples the mechanical vibrations from the converter to the horn and depending on its size and shape, can increase or decrease the amplitude of these vibrations.

The horn transmits the vibrational energy from the booster into the workpiece. The horn design is critical, since, like the booster, its size and shape affect the amplitude of the vibrations and consequently the heating of the parts.

The booster and the horn amplify the longitudinal vibrations generated by the transducer. The booster also serves as mounting for the entire stack, at which either a torque or a linear downward force is applied, so that the horn is pressed onto the parts. For metal welding the ultrasonic energy is transmitted into the workpieces via the transverse vibration occurring at the tip of the welding horn. The amplitude of vibration at the workpieces varies by system, tool design and power settings for a given application. Typically amplitude is in the range of 10 to 100 microns, peak-to-peak.

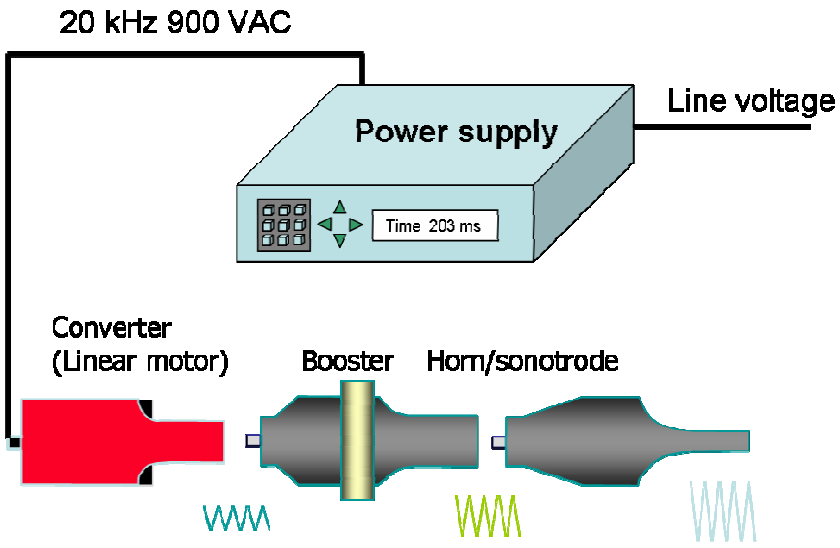

Figure 2 Illustration of ultrasonic metal welding system (Picture by Branson Ultrasonics)

The selection of a particular welding frequency is primarily determined by the application size. Typically higher frequencies produce higher relative velocities, thus higher frequencies can dissipate high powers (for given amplitude). However, because the converter is designed to resonate at the welding frequency, the available power from higher frequency units is limited. Thus, only smaller parts, such as small diameter tubing or micro-electronic inter-connections are welded at higher frequencies (>40 kHz). Larger applications requiring higher power are typically welded at lower frequencies (~20 kHz) where large, higher power converters can be designed. Frequencies below 20 kHz are typically not used, because in order to dissipate reasonable power levels, the amplitude must be relatively high and part damage can occur.

During welding, the machine control is usually set to a particular mode. For example, for the energy mode, the power supply will monitor the power and integrate the value over time. Once a preset amount of energy is dissipated, the power supply

discontinues the ultrasonic energy, independent of the time. In contrast, in the time mode, the sonics remain on for a present length of time, independent of the energy. In the last mode, post height, the power supply monitors an encoder on the actuator and continues to apply ultrasonic energy to the parts until the preset amount of post height (displacement) occurs.

It is important to note that it is an industry standard to use an energy mode for process control.

It is possible to make a very simple model of the weld process by assuming two interfaces rubbing together at pre-selected amplitude as seen in Figure 3.

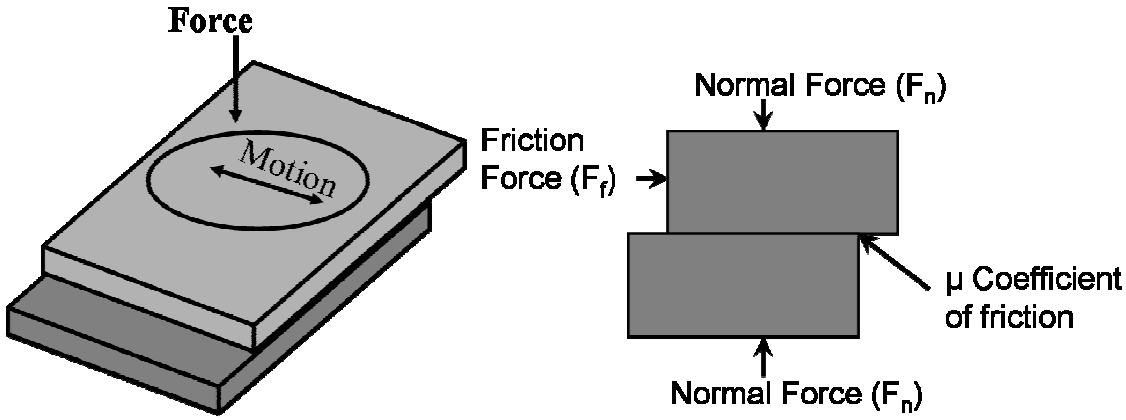

Figure 3 (a) Cartoon of welding showing LOCAL motion (b) small element removed from center of (a)

If it is assumed:

1) No losses on motion within the sample

2) The lower part remains perfectly stationary

3) Constant material properties

4) Constant displacement and forces

5) No inertial effects

6) No stored energy

The power (*P*) can be defined in terms of the frictional force (F) and the velocity as:

$$P = F \bullet v \qquad \text{[Eq. 1]}$$

In addition, the instantaneous velocity (v) can be defined as:

$$v(t) = A_0 \omega \cos(\omega t) \qquad \text{[Eq. 2]}$$

if it is assumed that the instantaneous displacement (*x(t)*) is defined as:

$$x(t) = A_0 \sin(\omega t) \qquad \text{[Eq. 3]}$$

Where A_0 is the peek displacement. Thus the instantaneous dissipated power can be defined as:

$$P(t) = F \bullet A_0 \omega \cos(\omega t) \qquad \text{[Eq. 4]}$$

Furthermore, it is possible to define the frictional force (F) as

$$F = \mu \cdot f \qquad \text{[Eq. 5]}$$

where μ is the dynamic coefficient of friction and *f* is the applied normal force. Thus, the instantaneous power is:

$$P(t) = f\mu A_0 \omega \cos(\omega t) \qquad \text{[Eq. 6]}$$

The average power (P_{avg}) can then be estimated by integrating this function of over a wave period and is defined as:

$$P_{avg} = \frac{2 f \mu A_0 \omega}{\pi} \qquad \text{[Eq. 7]}$$

Amplitude profiling

The amplitude in ultrasonic metal welding is defined as the peak-to-peak displacement of the horn at its work face as expressed in μm or in. The amplitude of the horn can be controlled electrically by adjusting the voltage to the converter. Evaluation of various weld control techniques has revealed that the use of amplitude profiling might provide a process benefit to welding aluminum. Amplitude profiling basically performs a weld using two different amplitude settings. Conventionally welds are made with a single pre-selected value. The first setting is called the "A" setting and the second setting is the

"B" setting. The trigger point for the A to B transition during the weld can be made with a number of methods such as: time, energy level and a peak power value. During the aluminum welding studies the trigger point method most commonly used is the time mode.

Profile typically starts with a high "A" amplitude and drops to a lower "B" amplitude with a trigger time of 0.2 seconds for the coupons of 2-mm thickness and 0.4 seconds for the coupons of 3-mm thickness. The process generally puts high amounts of power into weld samples during the "A" amplitude phase and drops the power input during the "B" phase, see Figure 4. In this case, the amplitude is profiled to match the various "stages" of the welding process. For example, the amplitude is relatively high at the start of the weld where the weld interface is solid/solid and requires significant velocities (amplitude) to promote heating and shearing/removing of the asperity peaks. At the end of the weld cycle, the amplitude is decreased to reduce shearing of the weld as the sample heats and softens. In addition, the lower amplitude reduces shearing of the forming weld, which reduces weld damage.

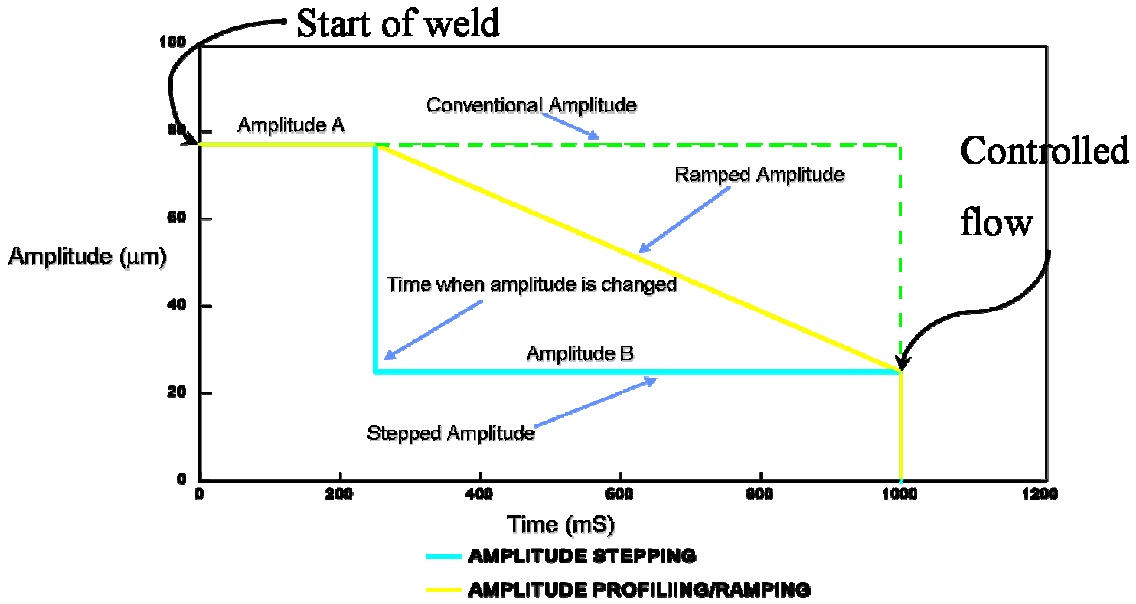

Figure 4 Example of amplitude profiling

Tooling

The ultrasonic stack assembly (see Figure 5) consists of: converter, booster, and horn.

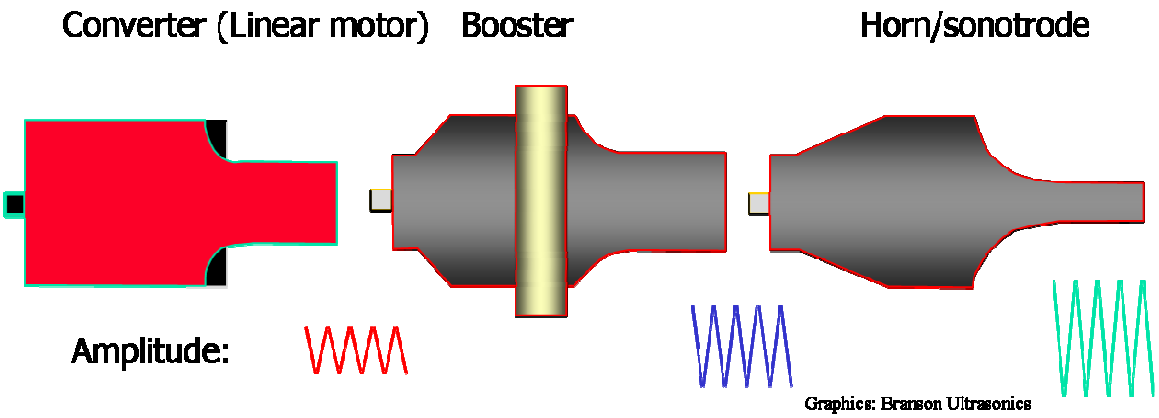

Figure 5 Details of stack assembly (image by Branson Ultrasonics)

The converter changes the electrical high-frequency signal from the power supply/generator into mechanical vibrations of the same frequency. To do this, the

converter uses piezoelectric elements which expand and contract (vibrate) when excited by the high-frequency voltage. The voltage is typically 900 VAC. An alternative technology to produce ultrasonic motion is magnetostrictive which relies on inducing physical changes in a material through the use of magnetic fields. This technology typically has low efficiency (<30%) due to high currents and resistive losses. Thus this technology is not detailed here. In order to assure high efficiencies, the converter is designed to resonate at the operating frequency and thus is typically ½ wavelength (λ) long. The booster and the horn are also typically designed to be a ½ wavelength long, however in some applications they are designed to be a multiple of ½ wavelength. The booster is a mechanical gain device that modifies the amplitude from converter. Typically the booster is designed to have a gain higher than 1 so that the amplitude from the converter is increased. For example, a typical 20 kHz converter can generate 20μm_{pp} of motion and thus with a 1:2.0 booster the amplitude at the booster face would be 40 μm_{pp}. The fundamentals of the booster are based on equilibrium of forces. At the nodal point (center of a ½ wavelength) of the booster, the sum of forces must be zero. As detailed in Figure 6 the force (F_1) on the side of the horn is M_1a_1 where $M_1$and a_1 is the total mass and acceleration on that side of the booster respectively. Thus, based on the summation of forces, the gain of the booster is simply the ratio of the masses on either side of the nodal point. The same principle also applies to the horn, which is often designed to further increase the amplitude. It is standard practice to hold the stack assembly at the nodal point of the booster since it corresponds to a location where there is no motion.

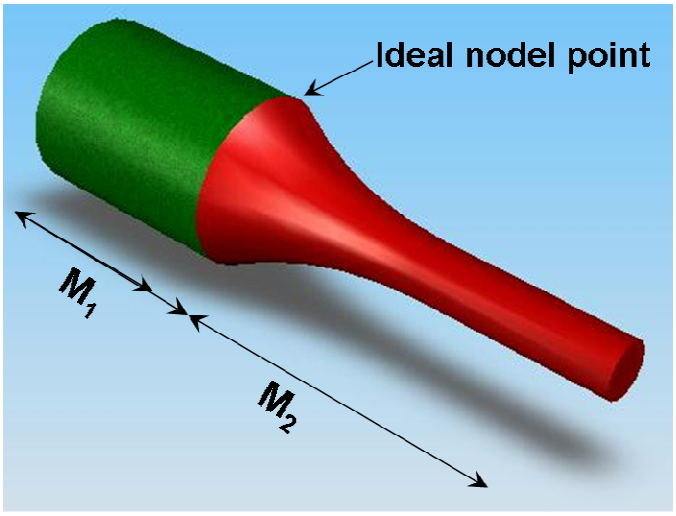

$$F = ma$$

From equilibrium :

$$F_1 = F_2 \Rightarrow m_1 a_1 = m_2 a_2$$

$$\frac{m_1}{m_2} = \frac{a_1}{a_2} = Gain$$

Figure 6 Details of a mechanical booster

For ultrasonic metal welding, the tip of the horn usually has a knurled or pattern design in order to promote interlocking of the horn to the top part. For example, Figure 7 shows a computer image of a "15 point" tip.

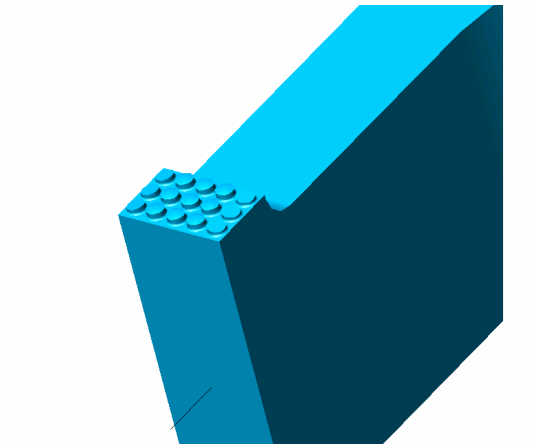

Figure 7 Computer generated image of a 15 point tool tip.

Joint design

An ultrasonic weld joint should incorporate four design characteristics:

- Alignment – Features such as pins and sockets, steps or tongues and grooves, should be provided to ensure repeatable alignment. Avoid using the horn and anvil to align the mating halves. When possible, provide features in the parts to align mating part halves rather than relying on the horn or fixture for alignment.
- Small contact areas – The initial mating surface contact area should be small to concentrate vibrations and decrease the time and energy needed to complete the softening. This also reduces horn marking.
- Uniform contact – The entire length of the joint surfaces should have uniform contact and be in one plane parallel to the horn face.
- Horn to joint distance – The distance between the horn contact surface and the weld interface should be less than 6 mm, whenever possible. While it is not formally defined for metal welding, in plastics welding the AWS (American Welding Society) refers to this as "near-field" welding. In contrast, when this distance is greater than 6mm it is considered far-field welding.

In ultrasonic metal welding these design characteristics are often not possible because of design constraints. For example, in welding sheet metal together for automotive body panels, the design is limited to simple lap shear joints with minimal features to reduce the weld profile as well as reduce manufacturing costs. Thus, in practice the final joint design is not optimized.

Research Questions

The research questions of this study are:

Research question 1

Does amplitude profiling improve the weld quality in terms of strength and appearance (reduction in part marking)?

Research question 2

Do buffer sheets of copper or zinc minimize the tool/part adhesion and improve the weld quality in terms of appearance and possibly weld strength?

Research question 3

Do any of the three control modes: energy, post height and time result in a change in weld consistency of strength?

Delimitations

Part marking and sticking of the specimens were characterized by visual examination and qualitative methods only, respectively.

Dissertation Organization

This dissertation consists of a general introduction to the study in Chapter 1, followed by three journal articles in Chapters 2, 3 and 4. Chapter 5 is a general discussion of the findings of the study and suggested future research.

Chapter 2, "The evaluation of the amplitude profiling in the ultrasonics welding of aluminum" details the benefit of using amplitude profiling over constant amplitude in the ultrasonic welding of aluminum. Also, the paper examines the difference between the experimental data and a theoretical model of dissipated power.

Chapter 3, "Evaluation of copper and zinc buffer sheets in ultrasonic welding of aluminum" studied the improvement of the part marking and tool/part adhesion by the addition of a thin sheet (~0.1-mm) of copper or zinc in between the tool (horn) and the top part prior to welding.

Chapter 4, "Comparison of control algorithms for ultrasonic welding of aluminum" statistically analyzes the difference between various control modes: energy, post height and time used in the ultrasonic welding of aluminum. The main objective is to conclude which one (if any) resulted in more consistent welds in terms of strength.

CHAPTER 2: EVALUATION OF AMPLITUDE PROFILING IN ULTRASONICS WELDING OF ALUMINUM

To be submitted to American Welding Society Journal

Maria Vlad, David Grewell

Abstract

Although the ultrasonic metal welding has many advantages including speed and efficiency, there are several limitations namely: tool/part adherence, part marking and the lack in the consistency and predictability of the weld strength. To resolve these issues, a series of experiments were conducted using a stepped amplitude (amplitude profiling) and constant amplitude. Thus the main objective of this work was characterize the use the amplitude profiling and determine if there are any benefits to its use in terms of weld strength and appearance. The resulting welds were analyzed and compared. The amplitude of the horn can be controlled electrically by adjusting the voltage into the converter. Conventionally welds are made with a single pre-selected amplitude value. During the aluminum welding studies the trigger point method used was time.

The amplitude profiling resulted in higher strength values (~8 kN) compared to the constant amplitude (~5.5 kN) and slightly more consistent welds. In addition, amplitude profiling resulted in relatively shorter cycle times when compared to welds made at constant low amplitude. It was also seen that the benefits of amplitude profiling were more pronounced with 2-mm thick samples compared to welds made with 3-mm thick samples. That is to say, amplitude profiling increased weld strength more with the 2-mm thick samples than with 3-mm thick samples.

It was also seen in this study, that very simple friction models were able to reasonably predict dissipated powers. While the model had many assumptions that over simplified the actual process, it was able to predict power levels within 20% of the experimental power levels. When this model was coupled with a simple one-dimensional heat flow, time dependent model, the predicted temperatures were very similar to reported values for the initial phase of the welding cycle. However, the model diverged from experimental values after the initial phase and it is believed that this was due to the over-simplified assumptions of the model, such as constant material properties.

Introduction and background

Ultrasonic metal welding, invented over 50 years ago, is a process that consists of joining two metals by applying ultrasonic vibrations under moderate pressures. The high frequency (20 kHz) vibrations locally soften the overlap zone between the parts to be welded, forming a solid-state weld through progressive shearing and plastic deformation. The oxides and contaminants are dispersed by the high frequency motion ("scrubbing") producing a pure metal/metal contact between the parts allowing the intermetallic bonds to take place. Beyer states that "Ultrasonic welding of metals consist of interrelated, complex processes such as plastic deformation, work hardening, breaking of contaminant films, fatigue crack formation and propagation, fracture, generation of heat by friction and plastic deformation, re-crystallization, and interdiffusion." [1]

As previously noted, ultrasonic metal welding is a solid state welding process and Wodara [2] has theorized the weld formation takes place in three stages. The first stage consists of drawing together the surfaces to be welded (faying surfaces), causing them to

align themselves, due to the applied normal stress. The second stage is represented by the activation of the atoms at the joining surfaces (i.e. dislocations take place) and their chemical (electron) exchange (a metallic bond formed). The third stage leads to the formation of a strong joint by the chemical exchange (diffusion) of atoms occurring between the metallic substances, both locally (weld interface) and in the surrounding areas (weld zone). Diffusion of atoms on a microscopic scale is due to the deformation of the unit cells and the high dislocation density. The three stages taking place during the bond formation are a continuous process within very short time intervals and are therefore difficult to distinguish. A more detailed description of the three stages follows.

In the first stage, as soon as the pressure and the force of the horn are applied, asperities are smoothed out and the surfaces are brought into close contact to each other. Most parts of the surfaces are still covered by oxide and contaminants that need to be dispersed by the plastic deformation of the surfaces. The surfaces in close contact allow van der Waals forces to form. If the metals to be welded have a high difference in hardness, the softer material deforms more than the harder one, in which case there are more dislocations generated at the softer material's surface. Thus, metallic bonds can take place by the exchange of the electrons existent between the surfaces of the dissimilar materials. [2]

In the second stage, intermetallic metallic bonds form due to the high number of atoms coming into contact with each other at the interface. A distance of 4 to 5 Å between the metal atoms allows the chemical/metallic bonds to form. Also, dislocation centers form due to plastic deformation, representing the origin of the third stage. The dislocation centers are the zones where the atoms in the crystal planes slip past one

another at a much lower stress level. Welding of two different materials influences the duration of the second stage. If similar metals are welded, the first stage proceeds directly to the third stage due to the simultaneous deformation of the surfaces and immediate formation of active (dislocation) centers. If the metals significantly differ in hardness, the formation of the active centers on the harder material's surface takes longer. Heat produced by internal and external friction can allow a phase change that will increase the deformability of the harder metal. [2]

The third stage following immediately after metallic bonding, consists of interactions between the joint metals that start in the overlap zone and then spread to adjacent areas. Due to the plastic deformation in the interface, the grain structures are typically altered. Elastically deformed zones coexist with plastically deformed regions causing residual stresses to form. After a short time, the residual stresses relax due to the elevated temperatures and the altering superimposed stresses caused by the ultrasonic vibrations. The relaxation process consists of atoms changing their functional locations in the crystal lattice structure. Besides relaxation, re-crystallization and diffusion processes take place in the structure as well. Diffusion processes have insignificant effect on the joint formation, but always it results in a stronger weld. Unfortunately, there is no explanation for this phenomenon by Wodara. [2] For the metals case, since there is no solubility in each other in the solid state, the interatomic interactions are the only ones responsible for the slightly less strong joints. The Institute of Materials Science and Engineering of the University of Kaiserslautern has conducted systematic investigations with Al-sheets and flexible Al-wires to understand the adherence and to reduce this effect. They concluded that the adherence of aluminum is due to high temperatures and

"can be avoided by intermittent welding, when possible on both sides of the joint" or by applying a TiAlN-coating to the horn tip or "using an interlayer". [3]

Edgar [4] developed a multi-physical model of ultrasonic metal welding that included interfacial shearing and deformation, frictional forces, inertial effects, attenuation, heat flow as well as process parameters. The model accurately predicted weld temperature and dissipated power and required numerical methods for most of the calculations. It is proposed here that very simple models may be used to make first order approximations for quick and simple estimations of power and temperatures. For example, it is widely accepted that a model developed by Stokes [6], can be used to model friction welding of plastics. While the heating mechanisms are similar, the processing parameters are rather different. For example, in ultrasonic metal welding, the amplitudes are typically less than 100 μm_{pp}. In contrast, with vibration/friction welding of metals the amplitude is in the order of 2-3-mm_{pp}. In addition, the frequencies are different, 20 kHz and 200 Hz for ultrasonic metal welding and vibration plastic welding respectively.

Stokes showed that it is possible to make a very simple model of the weld vibration welding process for plastics. He assumed two interfaces rubbing together at a pre-selected amplitude (A_0) as seen in Figure 8. It is important to note that this motion is very similar to ultrasonic metal welding.

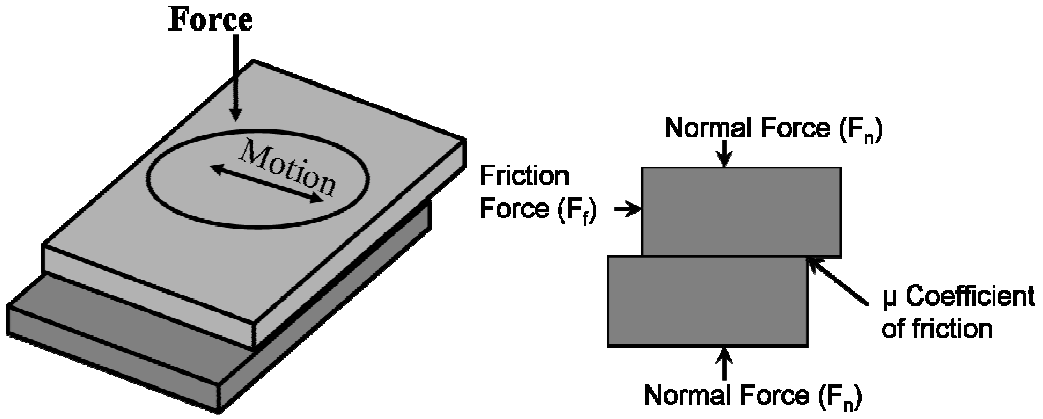

(a)

Figure 8 (a) Cartoon of welding showing LOCAL motion (b) small element removed from center of (a)

If it is assumed:

1) No losses on motion within the sample

2) The lower part remains perfectly stationary

3) Constant material properties

4) Constant displacement and forces

5) No inertial effects

6) No stored energy

The power (P) can be defined in terms of the frictional force (F) and the velocity as:

$$P = F \bullet v \qquad \text{[Eq. 1]}$$

In addition, the instantaneous velocity (v) can be defined as:

$$v(t) = A_0 \omega \cos(\omega t)$$ [Eq. 2]

if it is assumed that the instantaneous displacement (*x(t)*) is defined as:

$$x(t) = A_0 \sin(\omega t)$$ [Eq. 3]

Where A_0 is the peek displacement. Thus the instantaneous dissipated power can be defined as:

$$P(t) = F \bullet A_0 \omega \cos(\omega t)$$ [Eq. 4]

Furthermore, it is possible to define the frictional force (F) as

$$F = \mu \cdot f$$ [Eq. 5]

where μ is the dynamic coefficient of friction and *f* is the applied normal force. Thus, the instantaneous power is:

$$P(t) = f \mu A_0 \omega \cos(\omega t)$$ [Eq. 6]

The average power (P_{avg}) can then be estimated by integrating this function of over a wave period and is defined as:

$$P_{avg} = \frac{2 f \mu A_0 \omega}{\pi} \qquad \text{[Eq. 7]}$$

In order to apply this model to metal welding, there are several modifications that must be considered. For example, in an internal report by Grewell [5], it was observed that the amplitude at the tip of the horn droops during the welding cycle. This droop was most evident at the tip of the horn where the web thickness was approximately 1.2 cm. For example, Figure 9 shows the data as reported from the DUPS (digital universal power supply) power supply. The motional voltage (real part of graph in upper left hand graph), at the converter remains constant. That is to say the motional voltage remains constant at approximately 900 V_{rms}. The laser vibrometer measurements at the back driver bolt of the converter confirmed that the amplitude does remain relatively constant. However, the power curve (upper right hand graph of Figure 9) shows that there is a noticeable droop in the power. This is often indicative of an amplitude droop. This same droop is also seen in the imaginary voltage (upper right hand graph). It is theorized that this data may be useful in determining when an amplitude droop occurs.

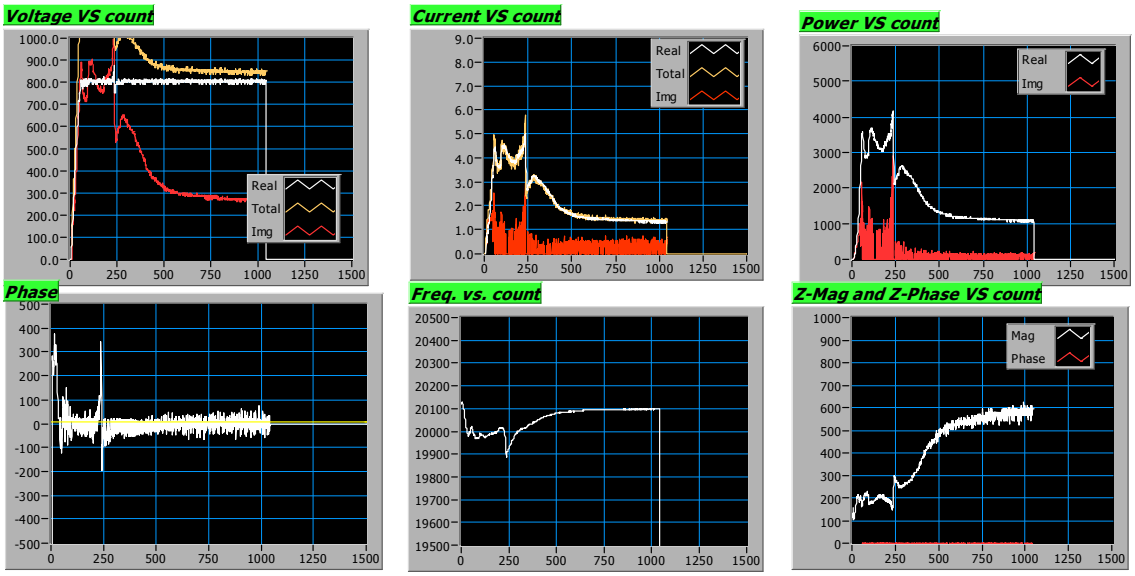

Figure 9 DUPS data for a typical weld cycle

In order to confirm the amplitude droop, the amplitude was measured at the horn tip during a weld cycle, as shown in Figure 10.

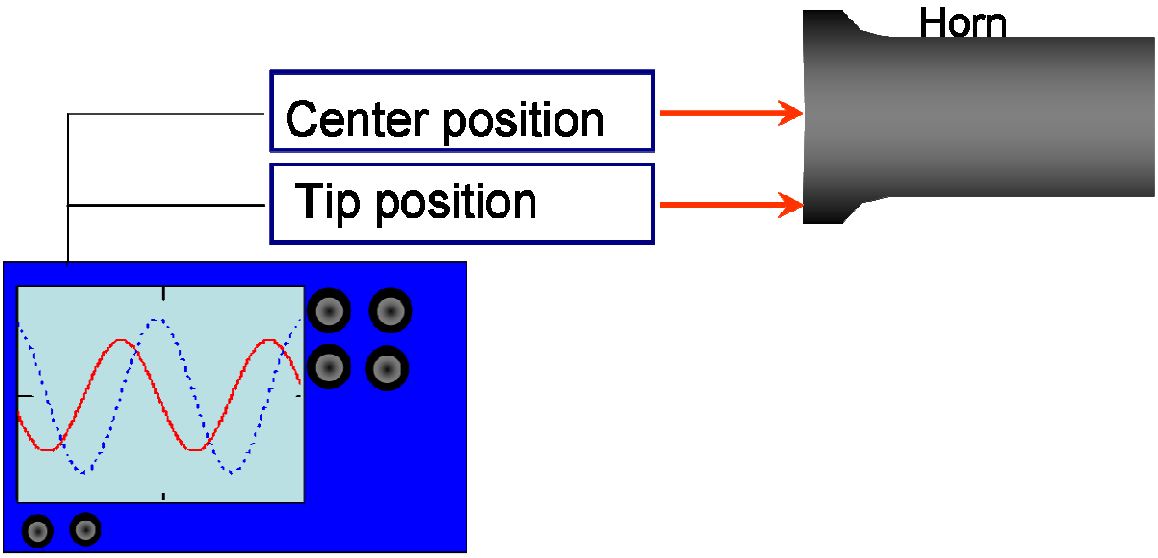

Figure 10 Details amplitude measurement at the horn tip

As shown in Figure 11, the amplitude droops from 55 μm_{pp} to 23 μm_{pp}. This is nearly a 60% amplitude droop.

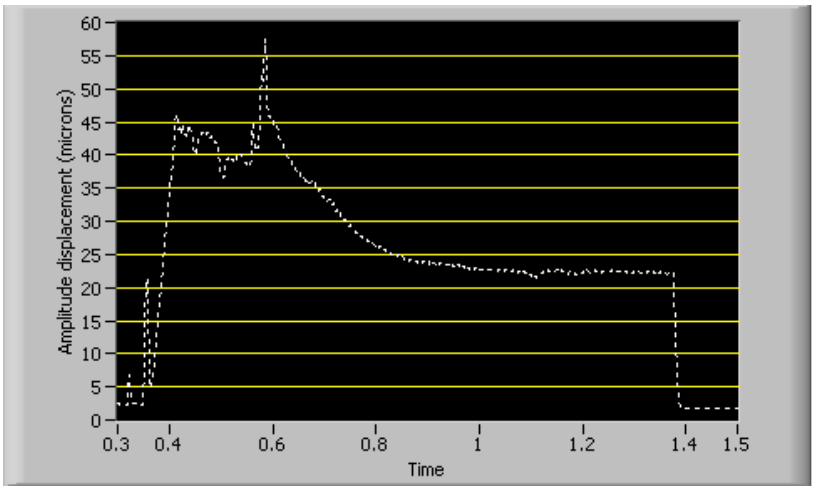

Figure 11 Amplitude (microns) at tip as a function of time (ms)

Amplitude measurements were also made at the center of the horn. As shown in Figure 12, the amplitude at the center of the horn remains relatively constant. Thus, it is believed the droop is localized to the tip.

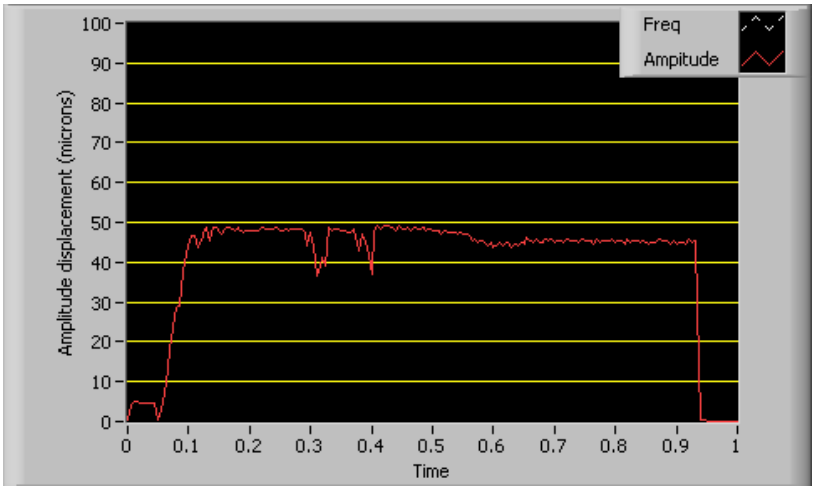

Figure 12 Amplitude (microns) at center of horn as a function of time (ms)

Thus, in order to apply Stokes' model, it will be estimated that the amplitude at the weld interface is approximately 50% of the initial amplitude. In addition, other non-standard assumptions must be applied for ultrasonic metal welding. For example, inertial effects must be assumed to be insignificant. While this is arguably false for ultrasonic welding, where the accelerations are high (+100,000 g's), Stokes model [6] does not include this affect in vibration welding where the acceleration is much lower (100 g's). Thus, one of the goals of this paper is to confirm if an over simplified model (Stokes' model) can be applied to ultrasonic metal and result in first order approximations.

In order to estimate maximum bond line temperature, we will make a huge assumption that we can use one dimensional heat flow model to predict the weld temperature as illustrated in Figure 13. This model will only work for the region that we are primarily interested in, that being where the temperature is the highest. It is expected that the point with the highest temperature to be at the center of the weld. By placing a coordinate system on top of that point, there is no temperature change in the y direction. So this model is only good for that very small region adjacent to the highest temperature point. And also in this model the heat flux across the weld interface is shown and we assume it to be uniform.

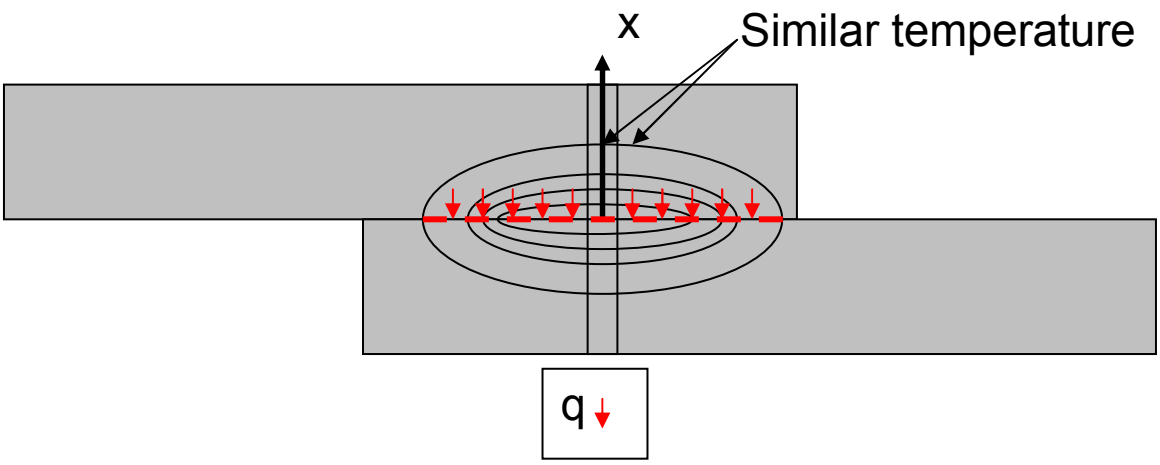

Figure 13 Illustration of the temperature model

In order to calculate the bond line temperature, the solution to the one dimensional heat flow differential equation was used. This solution is in terms of distance, time, and heat flux [Eq. 8]. While it is fully understood that the weld interfacial temperature is a function of distance (r) from the weld center line, it is argued that at the weld center line, symmetry allows us to assume heat flow in one direction based on the solution of the differential [Eq. 8].

$$\theta(x,t) = \theta_i + \frac{2 \cdot \dot{q}_0}{\lambda}\left[\sqrt{\frac{\kappa \cdot t}{\pi}} \cdot \exp\left(-\frac{x^2}{4 \cdot \kappa \cdot t}\right) - \frac{x}{2} \cdot \operatorname{erfc}\left(\frac{x}{2\sqrt{\kappa \cdot t}}\right)\right] \quad \text{[Eq. 8]}$$

Where θ is the temperature, x is the position, t is time, θ_i is the initial temperature of the solid, $\dot{q}_0$ is the heat flux at the surface, λ is the thermal conductivity, κ is the thermal diffusivity and $\operatorname{erfc}(z)$ is the complementary error function. The last assumption that must be considered in order to use this over simplified model is the size

of the weld. For example, it is well known that the weld size is a function of time, but by only considering the maximum temperature as reported by Edgar [4], we may be able to consider the final size of the weld. This size will allow us to estimate the cross-sectional area (A) for the weld. This then allows us to estimate the heat flux; $\dot{q}_0$=P/2A, at the surface (x=0), where it is reasonable to assume the maximum bond line temperature occurs. It is important to note that the power (*P*) is divided by two, because we assume the heat flows in both directions.

Ultrasonic metal welding has the advantage of having a relatively short cycle time (<2s), but its disadvantage are the tool/part adhesion and the part marking. This paper evaluates a method to improve these disadvantages by using amplitude profiling instead of constant amplitude.

The amplitude in the ultrasonic metal welding is defined as the peak-to-peak displacement of the horn at its work face as expressed in μm or in. The amplitude of the horn can be controlled electrically by adjusting the voltage into the converter. Evaluation of various weld control techniques has revealed that the use of amplitude profiling might provide a process benefit to welding aluminum. Amplitude profiling basically performs a weld using two different amplitude settings. Conventionally, welds are made with a single pre-selected value. In the case of amplitude profiling, the first amplitude setting is called the "A" setting and the second setting is the "B" setting (relative to a controller with a Product code WPC-1 From Branson Ultrasoniocs). The trigger point for the A to B transition during the weld can be made in a number of methods such as time, energy level and a peak power value. During the aluminum welding studies, the trigger point was

based on time. The selection of the mode was primarily determined based on experience and the fact that this is an industry standard as a starting mode during equipment setup.

Profile typically starts with a high "A" amplitude and drops to a lower "B" amplitude with a trigger time of 0.2 seconds for the coupons of 2-mm thickness and 0.4 seconds for the coupons of 3-mm thickness. The process generally dissipates high amounts of power into weld samples during the "A" amplitude phase and drops on the power dissipation during the "B" phase, see Figure 14. In this case, the amplitude is profiled to match the various "stages" of the welding process. For example, the amplitude is relatively high at the start of the weld where the weld interface is solid/solid and requires significant velocities (amplitude) to promote heating. At the end of the weld cycle, the amplitude is decreased to reduce heating and softening of the sample. In addition, the lower amplitude reduces shearing the forming weld to reduce weld damage.

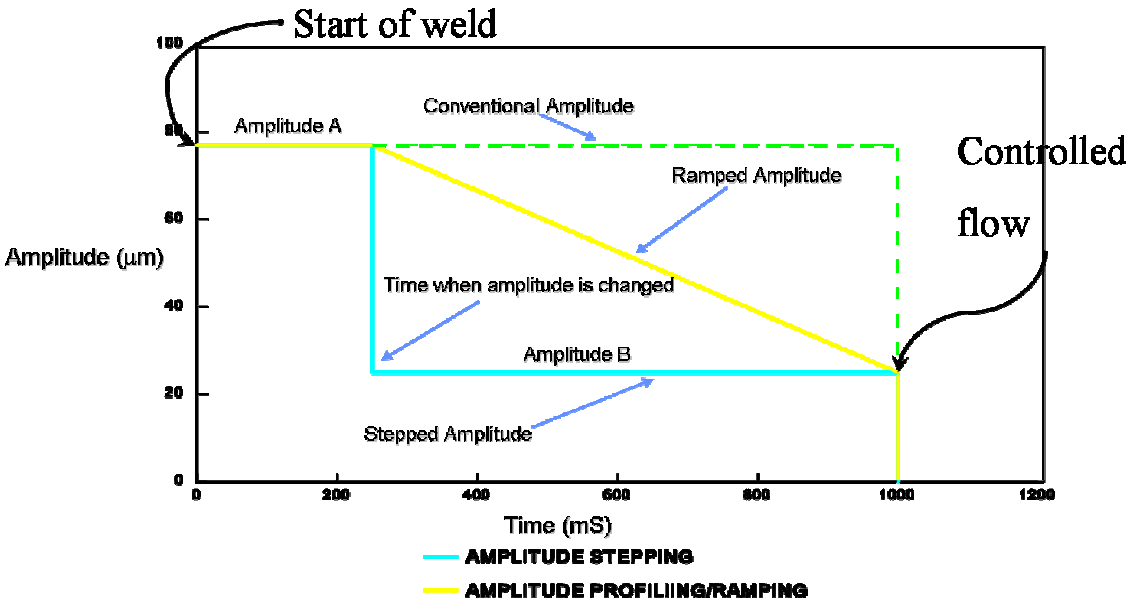

Figure 14 Example of amplitude profiling

Objective

The main objective of this work was to characterize the use of the amplitude profiling and determine if there are any benefits to its use in terms of weld strength and appearance. A second goal of this work was to determine if simple models based on frictional heating coupled with one dimensional heat flow models could accurately predict bond line temperatures. This objective would allow simple calculations that could be performed with standard software packages (Excel) to predict over aging and peak bond line temperatures.

Experimental procedure

Experimental design

Welds were made at various energy levels, where the energy level was calculated by the power supply. In this case the power supply digitally integrated the power curve and the sonics remained active until the preset level of energy was dissipated. The typical range of preset energy levels was between 500 and 5500 J, with increments of 500J depending on the weld quality and the equipment capacity. For example, if the energy level was too low, the weld was not complete, and if the energy level was too high, part marking was excessive and the power supply frequently overloaded. This range was selected based on screening experiments and experience. Ten welds were made with each energy level in increasing order of the weld energy level setting and were not randomized. The power level was 11, adding up to a total of ~110 samples for each amplitude setting. Weld amplitudes that were studied ranged from 40 to 60 μm_{pp}.

Additional details of the amplitude settings are defined in the *equipment* section. The weld force was set to a constant value of approximately 3400 N.

Materials

The ultrasonic metal welding was completed with aluminum 5754 coupons of two different thicknesses: 2-mm and 3-mm. The 5754 aluminum alloy was used as received, in the O-temper condition. Large sheets (~30 cm x 30 cm) sheets were provided by Ford Motor Company and the sheet sheared to produce 25.4 mm x 100 mm samples (1" x 4" in). The typical chemical composition for the 5754 aluminum alloy is: 2.6-3.2% Mg, 0.5% Mn, 0.4% Fe, 0.4% Si, the balance being aluminum. The weld sample configuration was a 25.4 mm x 102-mm and the weld configuration will be a 25.4 mm (1 in) overlap with the weld at the center of the over lap.

Equipment

The weld amplitude was varied using a WPC-1controller manufactured by Branson Ultrasonic Corp. The controller has the ability to vary the amplitude profiling at two separate values (A and B) with various switch over modes. The switch over mode is the parameter that defines when the amplitude is switched from value A (typically 60 μm_{pp}) to B (typically 43 μm_{pp}). For example, the mode can be set to time, energy and peak power. In this work only time was evaluated as this is the simplest mode to visualize and decouple from other welding parameters. In screening experiments, different amplitudes (50 and 58 μm_{pp}) were also studied, but the resulting weld strength and

consistency was lower (~3000N) than the ones described in this paper. The welding system was supplied by Branson Ultrasonic Corp. It consisted of a DUPS (Digital Universal Power Supply) power supply and had software that enabled recording the amplitude (motional voltage) and the dissipated power. The horn was a standard knurled tip as shown in Figure 15. The anvil was a standard "flex" anvil also detailed in Figure 16. The weld force was held constant at approximately 3360 N (750 lbs). A squeeze time of 0.2 seconds was used to allow the force to fully develop prior to activation of the sonics. The actuator was a specially designed pneumatic linear system that had linear rail to reduce rotation of the stack assembly during welding.

Figure 15 Picture of the horn

Figure 16 Picture of the anvil knurl pattern (Anvil tip)

Characterization

All welds (10 samples for every energy level) were tested in tension at a cross head speed of 10 mm/min. The maximum sustained load was used to calculate the ultimate strength. The testing method is shown in Figure 17. It is seen that shims were not used in the grips with the sample and thus bending stresses were not minimized.

Figure 17 Picture of the testing equipment while measuring the weld strength

Results and discussion

Figure 18 shows power as a function of time for the theoretical model described in the introduction and the power data obtained experimentally for three typical weld cycles during the ultrasonic aluminum welding using a constant amplitude of 43 μm. It is seen that the experimental power graph has a high peak value at the beginning of the weld and then drops. It is believed that this is the result of softening of the samples which attenuate the ultrasonic energy and reduce the effective amplitude at the faying surface. This reduction of amplitude then reduces the dissipated power. This effect is not

accounted for by the model, which explains the deviation in the theoretical and experimental power dissipation at the later stages of the weld. However, in general there is reasonable agreement between the two power curves.

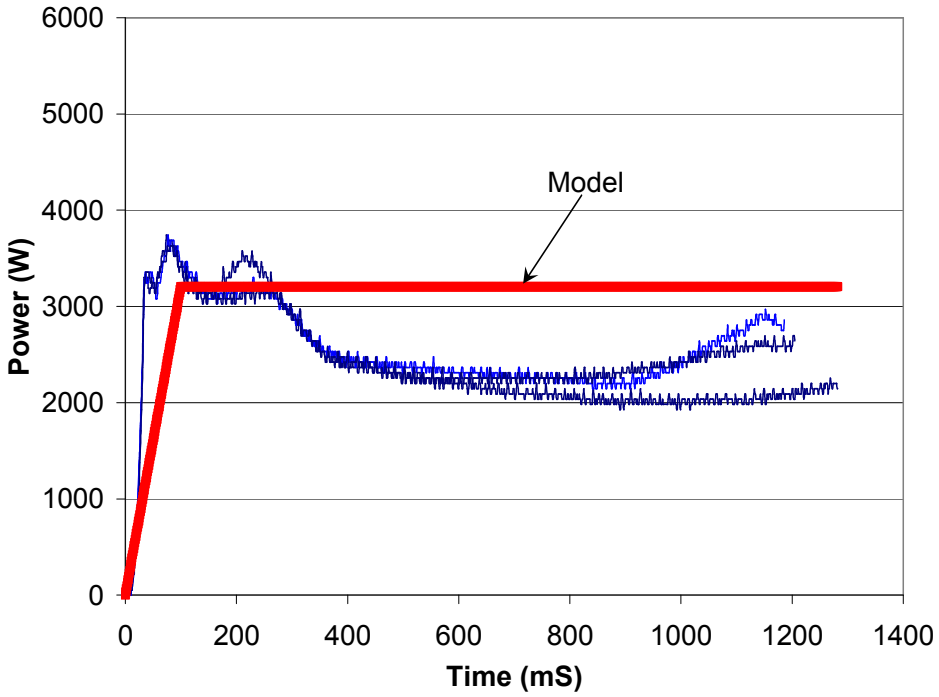

Figure 18 Measured and calculated power for 3 welds made with 43 µm amplitude

Figure 19 shows power as a function of time with a constant amplitude of 50 µm for the calculated power and the measured power. Again, it is seen that the experimental power starts with a high peak and it drops as the weld cycle proceeds. Interestingly it is seen that in one of the three welds studied, the power fluctuates as a function of time. It is believed that this is result of weld formation and shearing of the weld. That is to say, unlike the study with the lower amplitude (Figure 18) the higher amplitude fractures the

weld and this fracture is seen as intermediate increases in the dissipated power. However, it can be seen that the model predicted the dissipated power reasonably well.

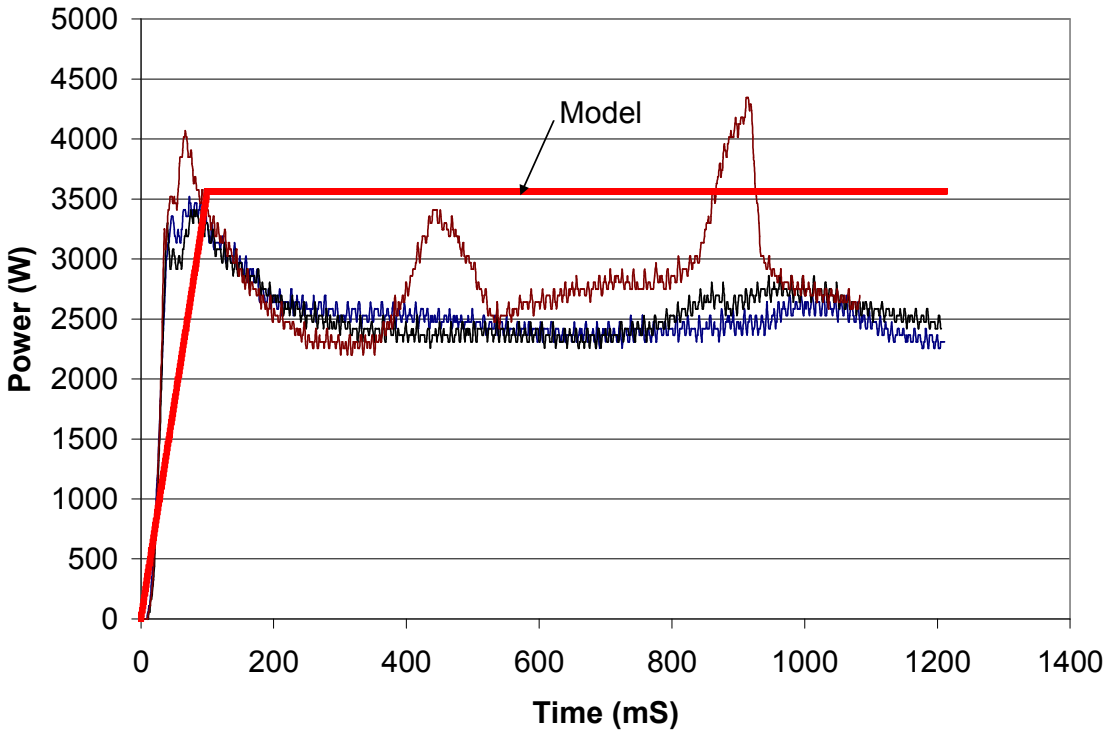

Figure 19 Measured and calculated power for 3 welds made with 50 μm amplitude

Figure 20 shows power as a function of time when amplitude profiling is used. Interestingly, power at the initial stage of the cycle did not flow in the same trend as previously noted. While there is no conclusive evidence to explain this observation, it is believed to be due to the sample variations. However, it is again seen that the model generally predicted the dissipated power reasonably well.

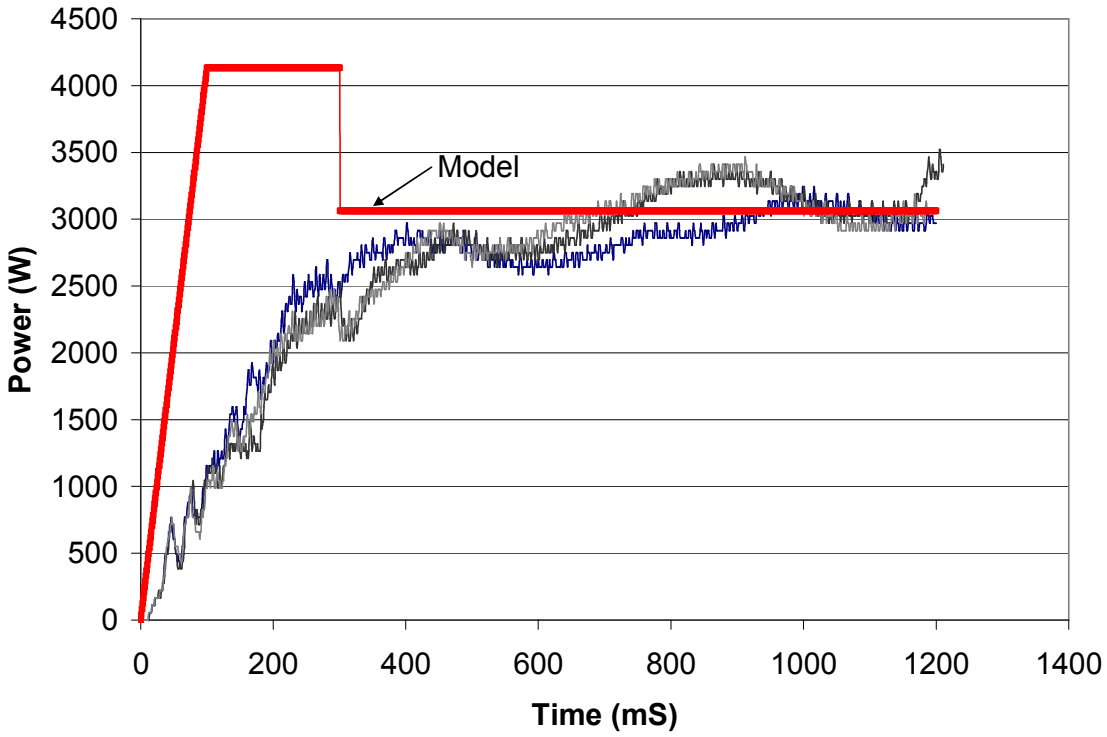

Figure 20 Measured and calculated power for 3 welds made with 58 to 43 μm amplitude

In order to validate the over simplified model, experimental data from Edgar [4] was used for verification. Edgar measured the typical bond line temperature with an IR-camera focused on a weld zone of a cross section weld. He found that the temperature was the highest at the faying surface but interestingly the maximum temperature occurred within the first 20-50 ms of the weld cycle. This is seen in Figure 21 where the maximum bond line temperature is plotted as a function of time for various welds made with condition similar to our study.

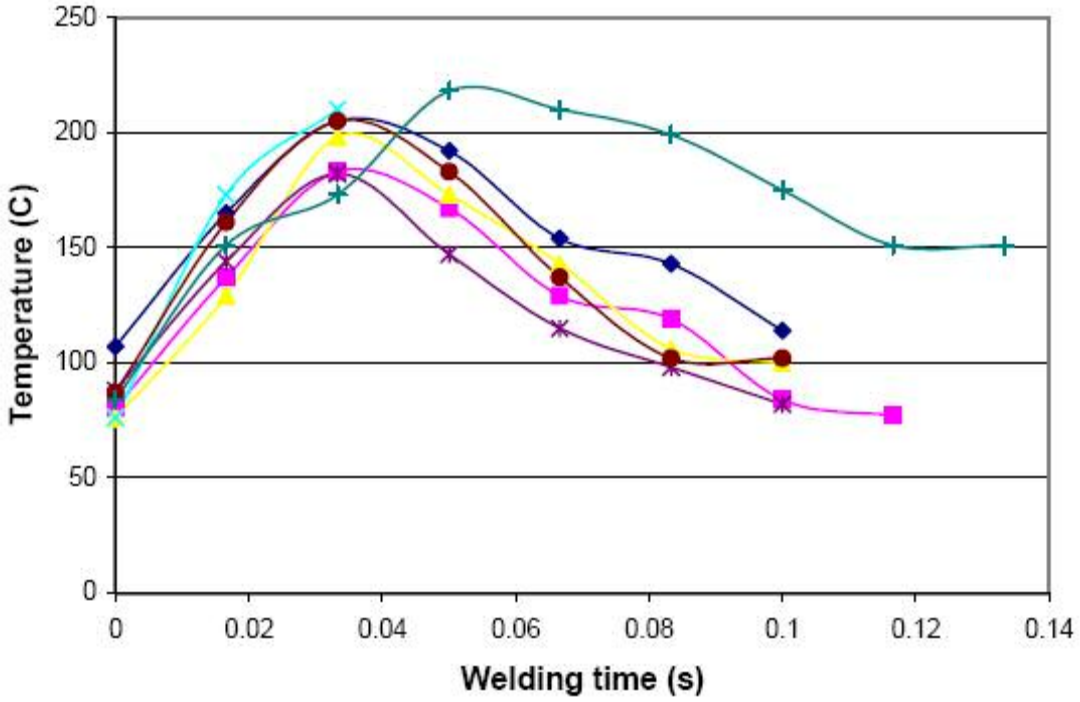

Figure 21 Experimental temperature data from Edgar's study [4] –different welding conditions

It is believed that the loss of heating that resulted in the drop in temperature beyond 60 ms is due to softening of the aluminum as well as amplitude droop as previously detailed. These two effects result in a drop of the amplitude at the faying surfaces and reduced the dissipated power (heat). Despite the experimental variations, Edgar [4] recorded peak temperature in the range of 200-300 °C.

Figure 22 shows the predicted weld zone temperature at various times as a function of distance from weld center line.

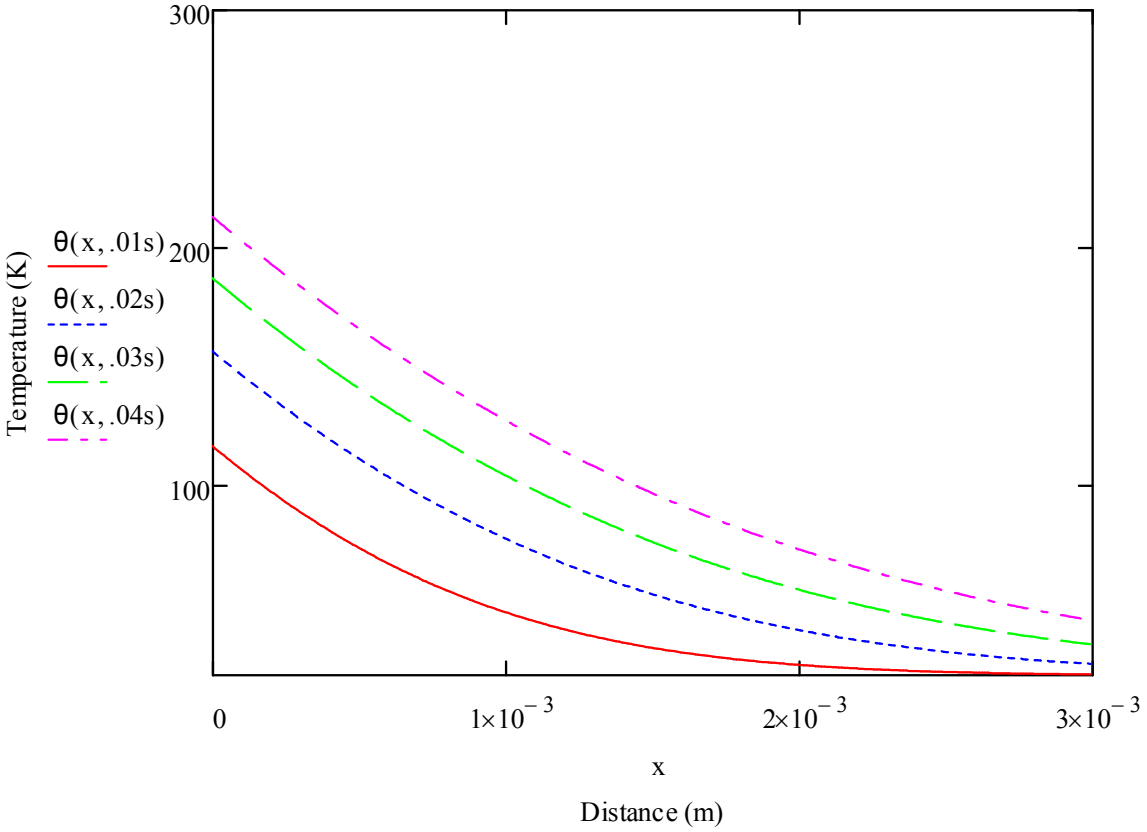

Figure 22 Temperature as a function of distance from center line at various heating times

It is seen that despite the simplicity of this model, the maximum temperature falls within the experimental values of Edgar's [4] work. It is important to note that with longer heating times, the model diverges from the experimental work and it is believed that this result of all the simplified assumptions. For example, the model assumes a semi-infinite body however, as seen in the graph above, at the edge of the sample (at x= 3-mm) the temperature is above the initial set value of 20 C. Thus, within the first 100 ms this assumption becomes invalid.

Amplitude profiling

Amplitude profiling experiments were conducted on coupons of 3-mm and 2-mm thickness and studying the weld strength as function of the preset energy values calculated as it was described in the introduction.

The study of the 2-mm 5754 coupons

In the studies evaluating the 2-mm-thick 5754 coupons, weld strength as a function of weld energy is seen in Figure 23. The benefits of using amplitude profiling of 60-43 μm over the constant amplitudes of 40 μm and 60 μm is seen. That is to say, with amplitude profiling there are slightly lower variations and higher values in terms of weld strength. In more detail, the amplitude profiling resulted in a maximum weld strength of over 6.0 kN. In comparison, the maximum weld strength achieved by using both constant amplitudes 40 μm and 60 μm was only slightly over 5 kN. It is important to note, that with amplitude profiling, a final amplitude of 40 μm was not used because of frequent power supply overloads. By slightly increasing the constant amplitude value to 43 μm, it was found that over loading could be eliminated. It is believed that because the welds are generally stronger with amplitude profiling, their stiffness is also generally higher. Thus, when the amplitude is reduced to 40 μm, the increased stiffness dissipates relatively higher power levels. It is important to note that the maximum power capacity of the power supply is directly proportional to the set amplitude level. It was observed that relative to the welding process, there is little difference between 40 and 43 μm.

It is important to note that the higher constant amplitude 60 μm resulted in higher standard deviation and more pronounced part marking and tool/part adherence compared

to the other amplitudes/profiles studied. Due to these problems, the 60 µm constant amplitude was not evaluated for the 3-mm thick samples. It was also noted that the weld time (cycle) for the welds made with amplitude profiling were typically less than 50% of the weld times for a given energy level for those welds made with a constant amplitude of 40 µm. This expected because of the relationship between power and amplitude.

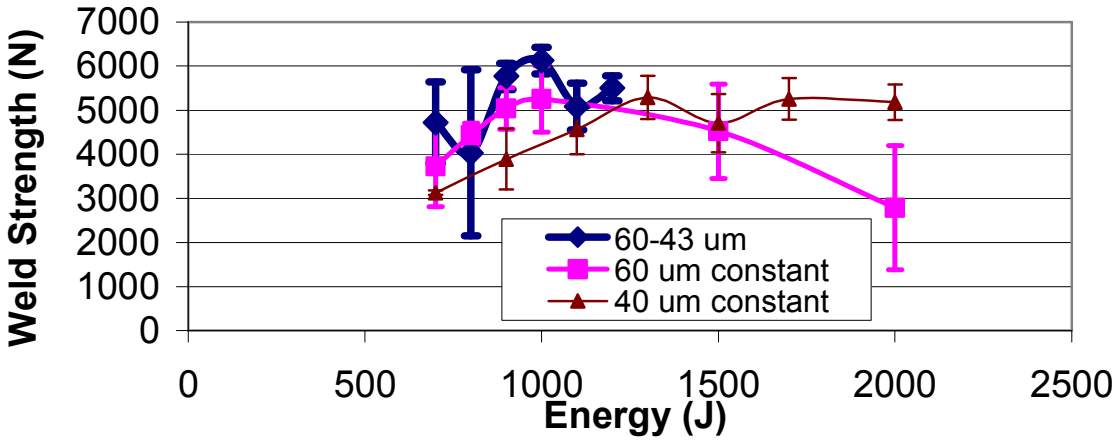

Figure 23 Strength vs. energy for amplitude profiling and constant amplitude for 2-mm coupons (um=µm)

The study of the 3-mm coupons of aluminum 5754

Figure 24 shows the weld strength as a function of weld energy for the welds made with 3-mm thick samples. There are several trends that can be seen in this graph. For example, the welds made with amplitude profiling of 60 to 43 µm had a relatively lower range of variation of the weld strength compared to those welds made with constant amplitude of 43 µm. The weld strength for the welds made with amplitude profiling was approximately ~8 kN, while in contrast the weld strength made with constant amplitude

was only approximately 5.5 kN. Again, the weld cycle time was reduced when amplitude profiling was used. Thus, it can be seen that there are benefits of the amplitude profiling in terms of the weld strength, weld strength consistency and cycle time.

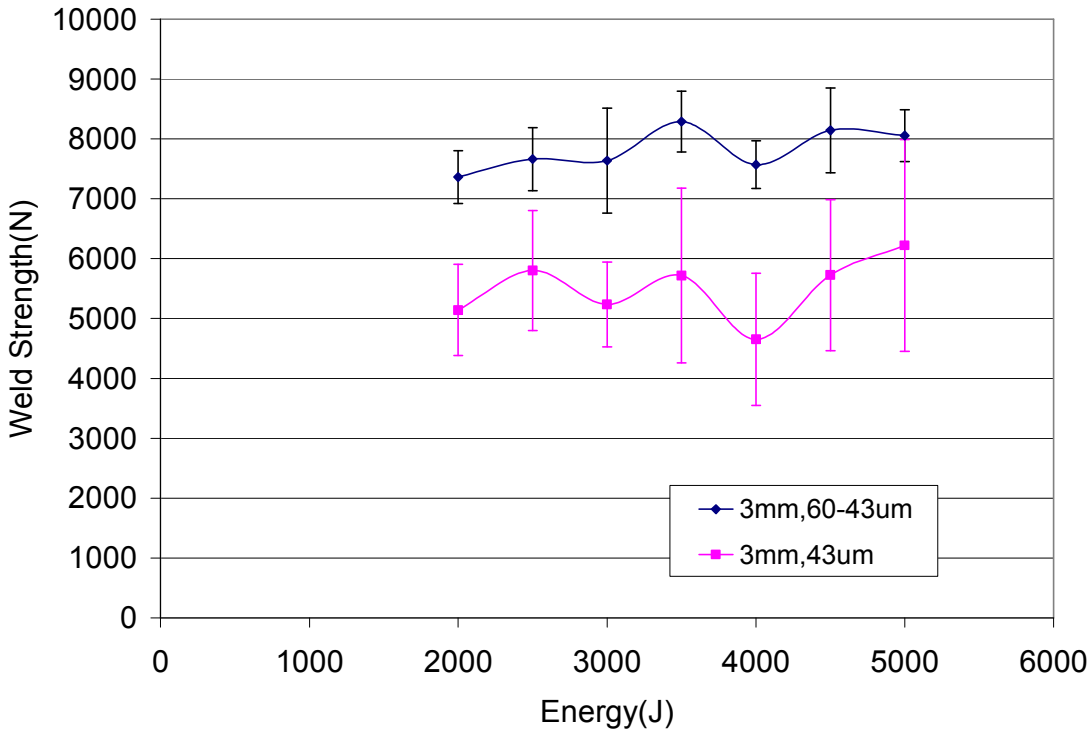

Figure 24 Strength vs. energy for amplitude profiling and constant amplitude for 3-mm coupons (um=μm)

In general amplitude profiling did not reduce the tool/part adhesion and part marking for both thicknesses (3-mm and 2-mm coupons of aluminum 5754 alloy) but it resulted in higher weld strength values and lower standard deviations, thus more consistent welds.

Because sticking appeared to occur randomly when making a series of welds, two welds with strength of ~8 kN were selected and characterized by optical micrographs;

one exhibited sticking and the other did not. The samples were cross-section cut, mounted, ground, polished and etched with different etchants.

Figure 25 shows the micrographs of the weld line of the sample that did not exhibit sticking. It is seen that the interface (faying surface) has incomplete fusion and in addition there are various large inclusions perpendicular to the weld line.

Figure 25 Micrograph of weld area of the non-sticking sample at 50x magnification

At higher magnification (1000x) and focusing on the same region (the fusion line) (Figure 26), it can be seen that there are precipitates (the black circles) around the grain boundaries as well as voids (the red circles). However, the number and size of voids appear to be limited.

Figure 26 Micrograph of weld area of the non-stick sample at 1000x magnification

Figure 27 shows the microstructure of the area adjacent to the tooling/horn region (near the horn/part interface). In the figure, the mirror image of the profile of the tip is seen and that the left edge is relatively smooth and only at the apex of the knurled surface is there evidence of fracture. It is believed that the fracture occurred during disengagement with the horn. Thus, because sticking was limited, the fracture (cracks below the surface) is also limited.

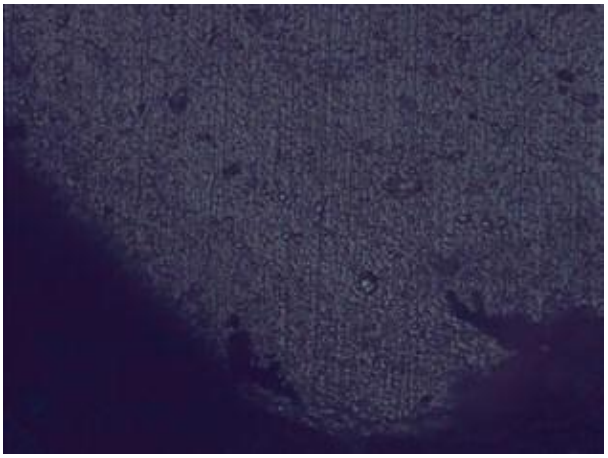

Figure 27 Micrograph of area underneath the horn of the non-stick sample at 1000x magnification

Similar micrographs of a sample that did exhibit sticking are seen in Figure 28. However, as seen in Figure 28, the weld line has larger cracks compared to the previous weld line that did not exhibit sticking. It is believed that these cracks are produced when the horn disengages from the parts; the forces that are produced because of the sticking, resulting in loading of the weld which produced the cracks. It is interesting to note, that while there are numerous cracks, the final weld strength was expected to be similar where sticking was not seen. However, because sample preparation was a destructive, there was no practical means of testing the actual weld strength for this particular weld. Thus, it is expected that this weld would have resulted in a relatively weld strength if it were tested.

Figure 28 Micrograph of weld area of the sticking sample at 50x magnification

One of the interesting artifacts of this weld is seen in Figure 29 to Figure 30. In these figures, there is evidence of large and numerous inclusions. While there is no evidence, it is believed that these inclusions were present in the base material prior to welding. Thus, it is believed that the base materials may have had different properties which resulted in sticking. Additional experiments are needed to confirm these results.

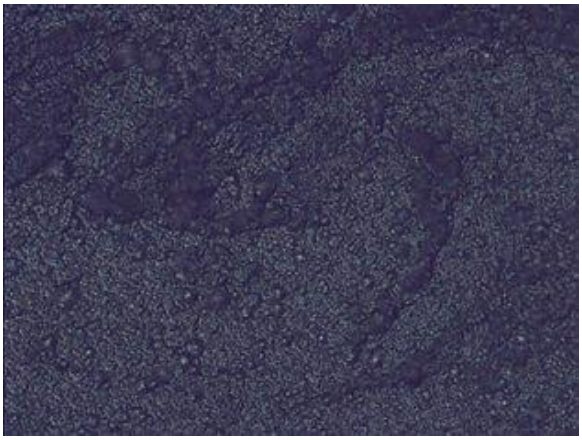

Figure 29 Micrograph of weld area of the sample with sticking at 1000x magnification

These inclusions are further seen at higher magnification in Figure 30.

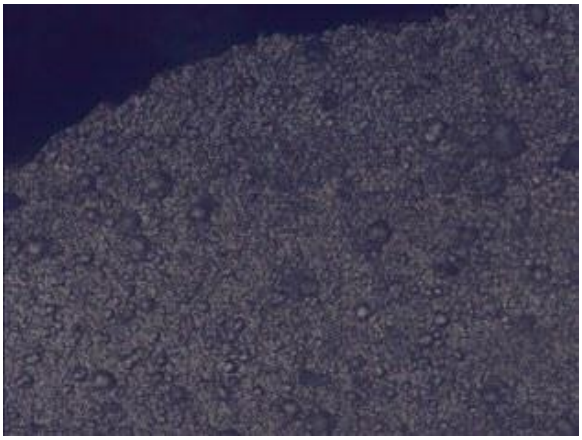

Figure 30 Micrograph of weld of sample with the sticking at 1000x magnification

Conclusions

In this study it was seen that over simplified models predicted the dissipated power within a range of 1000 W during ultrasonic metal welding. Measured power levels were in the range of 2000 to 3000 W and the models, based on friction and velocity, predicted power levels of 3000W. In addition, simple one-dimensional heat

flow solution accurately predicted bond line temperature for the initial phase of the weld. However, after softening of the sample, the model over predicted the temperature.

It was also seen in this study that amplitude profiling allows better matching of amplitude to the various phases of the weld. For example, by initiating the weld with a relatively high amplitude, fast heating and efficient welding can be promoted. Once the material is softened, the amplitude can be reduced to minimize shearing of the weld. Thus, amplitude profiling increases weld strength and reduces weld time. However, it was seen that the amplitude profiling did not affect the tool/part adhesion, thus there was no noticeable improvement of the horn adhesion to the top part during welding.

Thus in summary:

- Over simplified models reasonably predicted the dissipated power during ultrasonic metal welding
- Simple one-dimensional heat flow solution accurately predicted bond line temperature for the initial phase of the weld
- Amplitude profiling allows better matching of amplitude to the various phases of the weld
- Amplitude profiling increases weld strength and reduces weld time

References

1. Beyer, W., *The bonding process in the ultrasonic welding of metals*, Schweisstechnik, Jan. 1969, v.19, n. 1, pp. 16-20.
2. Wodara, J., *Joint formation in the Ultrasonic welding of Metallic Substances*, ZISMitteilungen, 1986, v.28, n. 1, pp. 102-108.
3. Gutensohn, M., Wagner, G., Eifler, D., *Reduction of the Adherence of Aluminum on Ultrasonic Welding Tools,* University of Kaiserslautern
4. de Vries, E., *Mechanics and Mechanisms of Ultrasonic Metal Welding*, *Dissertation,* Ohio State University, 2004.
5. Grewell, D., *Study on amplitude droop*, Branson Co.
6. Stokes, V.K., *Vibration welding of Thermoplastics*. Part I, *Polymer Engineering and Science*, June, 88, Vol. 28, No. 11, Society of Plastics Engineers, Brookfield, CT.
7. Rohsenow, W.M., Choi, H., *Heat, Mass, and Momentum Transfer* (1961) Prentice-Hall, Englewood Cliffs, N.J

CHAPTER 3: EVALUATION OF COPPER AND ZINC BUFFER SHEETS IN ULTRASONICS WELDING OF ALUMINUM

To be submitted to American Welding Society Journal

Maria Vlad, David Grewell

Abstract

Ultrasonic metal welding has many advantages including, short cycle times, efficiency and long tool life. It also has several limitations, namely consistency of the tool/part adherence, part marking and the lack in the consistency and predictability of the weld strength. To resolve these issues, a series of experiments were conducted using buffer sheets of copper or zinc between the tool (horn) and the coupons to be welded. The main objective of this work was to characterize the use of buffer sheets to reduce part marking and sticking between the horn and sample. The results were analyzed and compared with the coupons welded without buffer sheets. The buffer sheets reduced the tool/part adherence (sticking) and part marking. The buffer sheets produced intermetallic bonds at the horn/part interface which enhanced the mechanical properties of weld samples and prevented softening of the part. It was seen that copper buffer sheets reduced the ultimate weld strength but this effect was not observed with zinc buffer sheets. In addition, part thickness affected the impact of the buffer sheets. For example, thicker samples (3-mm) had a greater loss in weld strength with the use of buffer sheets compared to thinner (2-mm) samples weld with buffer sheets.

Introduction and background

Ultrasonic metal welding invented over 50 years ago is a process that consists of joining two metals by applying ultrasonic vibrations under moderate pressure. The high frequency vibrations (20 kHz) locally soften the overlap zone between the parts to be welded forming a solid-state weld through progressive shearing and plastic deformation. The oxides and contaminants are removed by the high frequency motion ("scrubbing") producing a pure metal/metal contact between the parts allowing the intermetallic bonds to take place. Beyer states that "Ultrasonic welding of metals consist of interrelated, complex processes such as plastic deformation, work hardening, breaking of contaminant films, fatigue crack formation and propagation, fracture, generation of heat by friction and plastic deformation, re-crystallization, and interdiffusion." [1] Also, it is worth mentioning that "The dominating mechanism for ultrasonic welding is solid state bonding, and it is accomplished by two different processes: Slip and plastic deformation." [1]

Because tool/part adhesion (stickage) and part marking are issues for manufacturing, finding a solution is critical in order to allow ultrasonic aluminum welding to be utilized in industry. Copper is known to improve the strength of the aluminum as an alloying element, if added in small quantities. [2, 3] By increasing the strength of the aluminum alloy, the risk of the horn tip penetration into the top part should be reduced. Also, by placing a Cu sheet between the horn tip and the top part prior to the ultrasonic welding, the tool/part adhesion should be greatly reduced because of the low steel/Cu affinity, as well due to the strengthening effect of Cu. [2, 3]

Figure 31 illustrates the buffer sheet placement and the part marking after the ultrasonic welding. It is seen that part marking is produced on both horn side as well as the anvil side, but the horn side has relatively more marking. Thus, the focus of this work was to improve the part marking at the horn interface only.

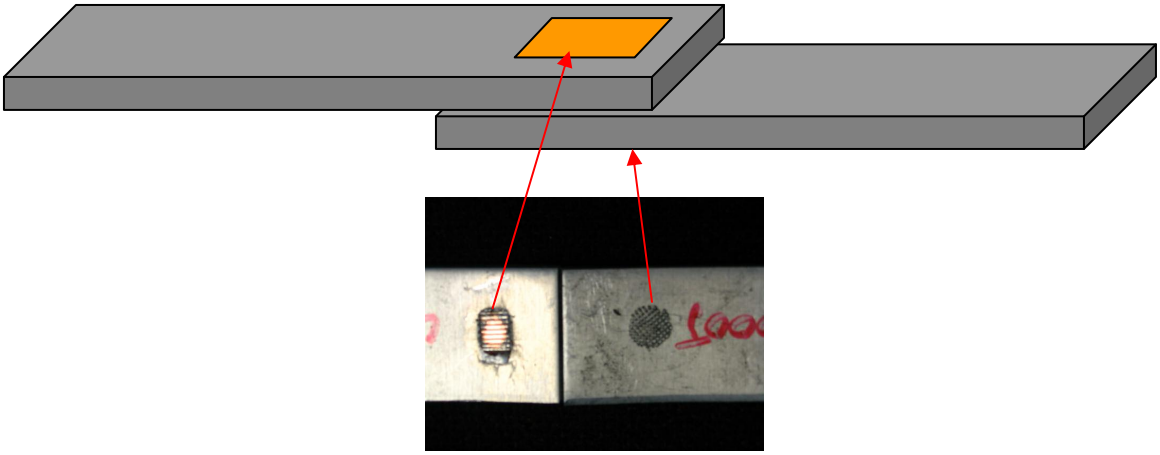

Figure 31 Buffer sheet placement on top and part marking at the bottom.

As previously noted, in addition to evaluating copper buffer sheets, zinc buffer sheets were also studied. Zinc was considered because of its reduced potential to promote galvanic corrosion. Galvanic corrosion is caused by the difference in the electrical potential of two metals in contact in the presence of an electrolyte, leading to the dissociation of the metal with a higher electrical potential [4] into the electrolyte. Since zinc's electrical potential value (+0.758 V) is close to aluminum's electrical potential value (+1.3 V), zinc's potential of promoting galvanic corrosion is relatively low. However, the difference between the copper electrical potential (-0.345 V) and the aluminum electrical potential (+1.3 V) is relatively high and could easily lead to galvanic corrosion in the presence of an electrolyte. [4]

Objective

The main objective of this work was to characterize the use of buffer sheets to reduce part marking and sticking between the horn and sample. This proposed solution would increase productivity and part quality in industry.

Experimental procedure

Experimental design

Welds were made at various energy levels, where the energy level was calculated by the power supply. In this case the power supply digitally integrated the power curve and the sonics remained active until a preset level of energy was dissipated. The typical range of preset energy levels was between 500 and 5500 J, depending on the weld quality and the equipment capacity. For example, if the energy level was too low, the weld was not complete, and if the energy level was too high, part marking was excessive and the power supply frequently overloaded. This range was selected based on screening experiments and experience. The welds were made in increasing order of the weld energy level setting with increments of 500J and were not randomized. Ten samples were welded for each energy level setting, adding up to a total of ~110 samples for each amplitude setting. Weld amplitudes that were studied ranged from 40 to 60 μm_{pp}. Additional details of the amplitude settings are defined in the *equipment* section. The weld force was set to a constant value of approximately 3400 N.

Materials

The ultrasonic metal welding was completed with aluminum 5754 coupons of two different thicknesses: 2-mm and 3-mm. The 5754 aluminum alloy was used in an as received condition, in the O-temper condition. Large sheets (~30 cm x 30 cm) sheets were provided by Ford Motor Company and the sheet sheared to produce 25.4 mm x 100 mm samples (1" x 4" in). The typical chemical composition for the 5754 aluminum alloy is: 2.6-3.2% Mg, 0.5% Mn, 0.4% Fe, 0.4% Si, the balance being aluminum. The weld sample configuration was a 25.4 mm x 100 mm and the weld configuration will be 25.4 mm (1 in) in overlap with the weld at the center of the overlap.

The use of inserting a Cu or Zn buffer between the horn and the two aluminum 5754 coupons to be welded, prior to the ultrasonic welding process was investigated. The study focused on the difference between the constant amplitudes (60 μm and 43 μm) and the amplitude profiling (60-43 μm) with and without buffer sheets and with buffer sheets of various thicknesses.

Equipment

The weld amplitude was varied using a WPC-1controller manufactured by Branson Ultrasonic Corp. The controller has the ability to vary the amplitude profiling at two separate values (A and B) with various switch over modes. The switch over mode is the parameter that defines when the amplitude is switch from value A (typically 60 μm_{pp}) to B (typically 43 μm_{pp}). For example, the mode can be set to time, energy and peak power. In this work only time was evaluated as this is the simplest mode to visualize and decouple from other welding parameters. In screening experiments, different amplitudes

(50 and 58 μm_{pp}) were also studied, but the resulting weld strength and consistency was slightly lower (~3000N) than the ones described in this paper. Welds were made at various energy levels, where the energy level was calculated by the power supply. In this case the power supply digitally integrated the power curve and the sonics remained active until a preset level of energy was dissipated. The typical range of pre-set energy levels was between 500 and 5500 J, depending on the weld quality and the equipment capacity. For example, if the energy level was too low, the weld was not complete, and if the energy level was too high, part marking was excessive and the power supply frequently overloaded. This range was selected based on screening experiments and experience.

The welding system was manufactured by Branson Ultrasonic Corp. The horn was a standard knurled tip as shown in Figure 32. The anvil was a standard "flex" anvil also detailed in Figure 33. The weld force was held constant at 3360 N (750 lbs). A squeeze time of 0.2 seconds was used to allow the force to fully develop prior to activation of the sonics. The actuator was a specially designed pneumatic linear system that had linear rail to reduce rotation of the stack assembly during welding.

Figure 32 Picture of the horn

Figure 33 Picture of the anvil knurl pattern (Tip)

Characterization

All welds were tested in tension at a cross head speed of 10 mm/min. The maximum sustained load was correlated the ultimate strength. The test configuration is shown in Figure 34. It is seen that shims were not used in the grips with the sample and thus bending stresses were not minimized.

Figure 34 Picture of the testing equipment

Results and discussion

The study of the 3-mm coupons of aluminum 5754 using 0.1-mm Cu buffer sheets

In those studies using a 0.1-mm thick Cu buffer sheets, weld strength as a function of energy graph is seen in

Figure 35. It is seen that at the relatively high amplitude 60 μm, the weld strength is relatively low and rarely exceeded 3000 N. It is believed that is due to shearing of the weld, which prevented proper fusion of the faying surfaces. In short, the shearing promoted fracture of the faying surface at the end of the cycle. With the lower amplitude of 40 μm and amplitude profiling 43 to 60 μm, the weld strength was typically over 4000 N. It is important to note that with amplitude profiling a final amplitude of 40 μm was not used because of frequent power supply overloads. By slightly increasing the constant amplitude value to 43 μm, it was found that overloading could be eliminated. It is believed that because the welds are generally stronger with amplitude profiling, their stiffness is also generally higher. Thus, when the amplitude is reduced to 40 μm, the increased stiffness dissipates relatively higher power levels. It is important to note that the maximum power capacity of the power supply is directly proportional to the set amplitude level. It is believed that relative to the welding process, there is no difference between 40 and 43 μm. In addition, at the lower amplitude the weld strength exceeded 6000 N with weld energy of 5500 J. It is believed that the lower amplitude allowed the weld to cool under low shearing promoting good fusion and the higher energy produced large welds. It is important to note that without amplitude profiling, the cycle times for the welds made with the lower amplitudes were typically 2 to 3 times longer.

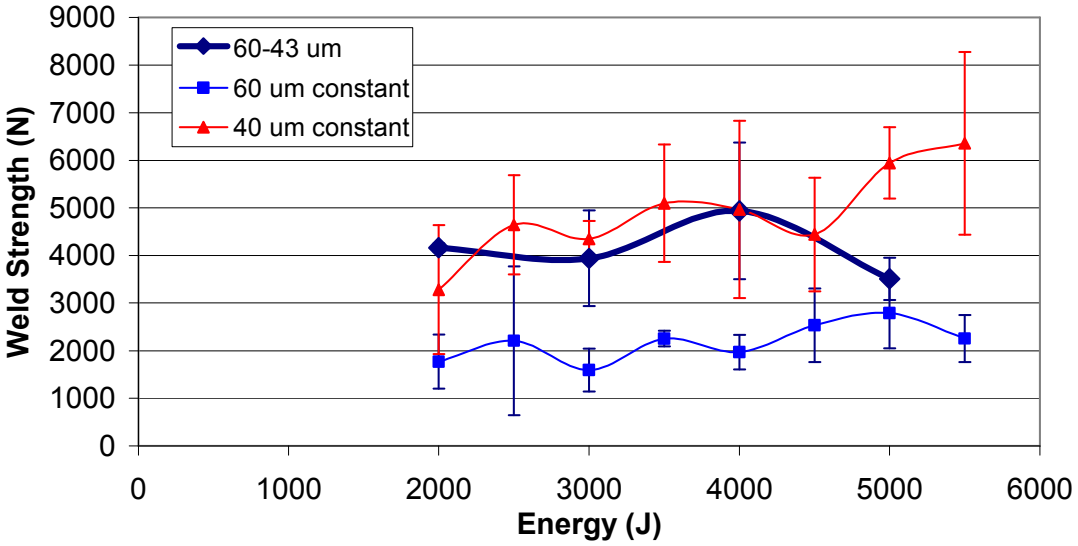

Figure 35 Weld strength with 0.1-mm Cu inserts -Strength vs. energy for amplitude profiling and constant amplitude for 3-mm coupons

Because amplitude profiling was seen to have some benefits to the ultrasonic welding of aluminum, such as relatively high weld strength, the following graph (Figure 36) shows the weld strength as a function of energy only for the amplitude profiling. The graph compares the weld strength values of the samples welded with and without 0.1-mm copper buffer sheets. It is seen that the maximum weld strength for the samples welded without buffers sheets was slightly over 8 kN. In contrast, the samples welded with 0.1-mm copper buffer sheets had a maximum weld strength of ~5 kN. It is important to note that the copper buffer sheets noticeably reduced the part marking and the tool/part adhesion as will be detailed shortly. Thus, the thick samples welded with 0.1-mm copper buffer sheets result in lower weld strength, but the part marking and the tool part adherence problems are minimized.

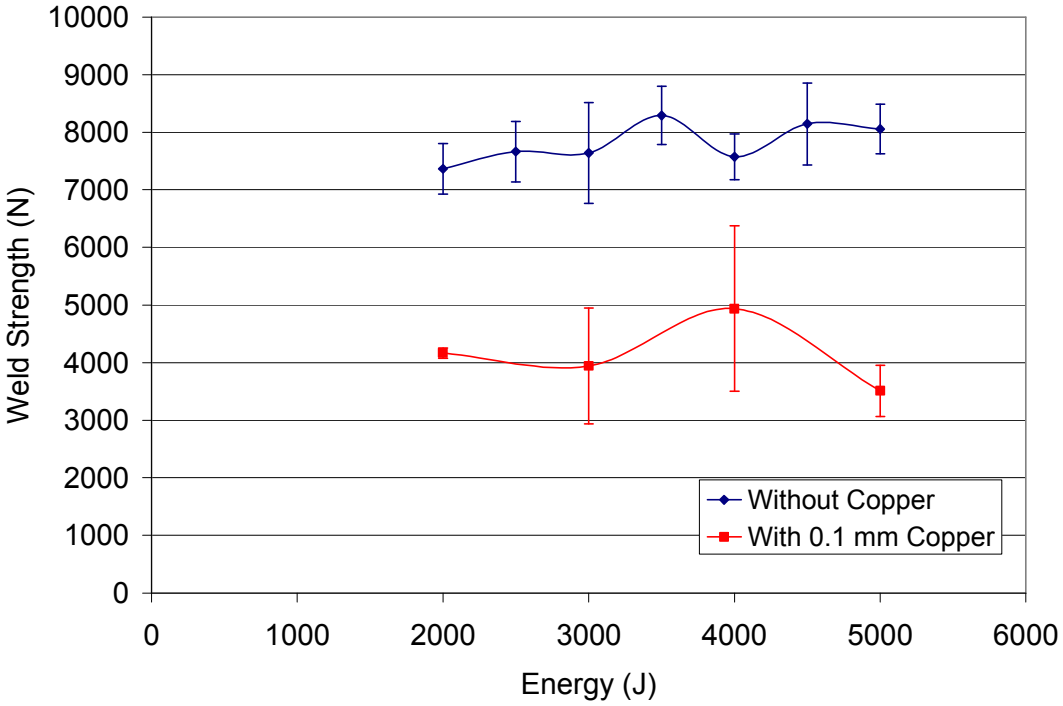

Figure 36 Weld Strength vs. energy with amplitude profiling with and without 0.1-mm copper for 3-mm samples

The study of the 2-mm coupons of aluminum 5754 using 0.1-mm Cu buffer sheet

In the studies using 0.1-mm Cu buffer sheets for the welding of 2-mm thick 5754 coupons, weld strength as a function of energy graph is seen in Figure 37. Interestingly, the welds made with thinner samples produced higher weld strengths compared to the previous results with the thick samples. For example, in the previously detailed experiments with thick samples, the weld strength typically never exceeded 5000 N. However, with the thinner 2-mm thick samples, it is seen that in many conditions, the weld strength exceeded 5000 N. It is believed that with the thicker samples (3-mm) the amplitude is attenuated and inertial effects reduce the true amplitude at the faying surface. In contrast, with the thinner samples, the amplitude is higher and thus welding is

more effective. This is supported by the observation that with the thinner samples and higher amplitude, where shearing of the fused joint promotes failure, the weld strength was typically only 1000 N and never exceeded 4000 N. It is also seen that amplitude profiling produced relatively high weld strengths. For example with constant amplitude of 40 µm, the maximum weld strength was less than 5000 N. Higher weld energies (>3000 J) with a constant amplitude of 40 µm experienced noticeable part marking and were excluded from this study. However, when amplitude profiling was utilized the weld strength was as high as 5500 N. In addition, when the copper buffer sheets were used, the sticking and the marking were greatly reduced. As previously noted, welds made with constant amplitude had cycle times 2 to 3 times longer compared to those welds made with amplitude profiling.

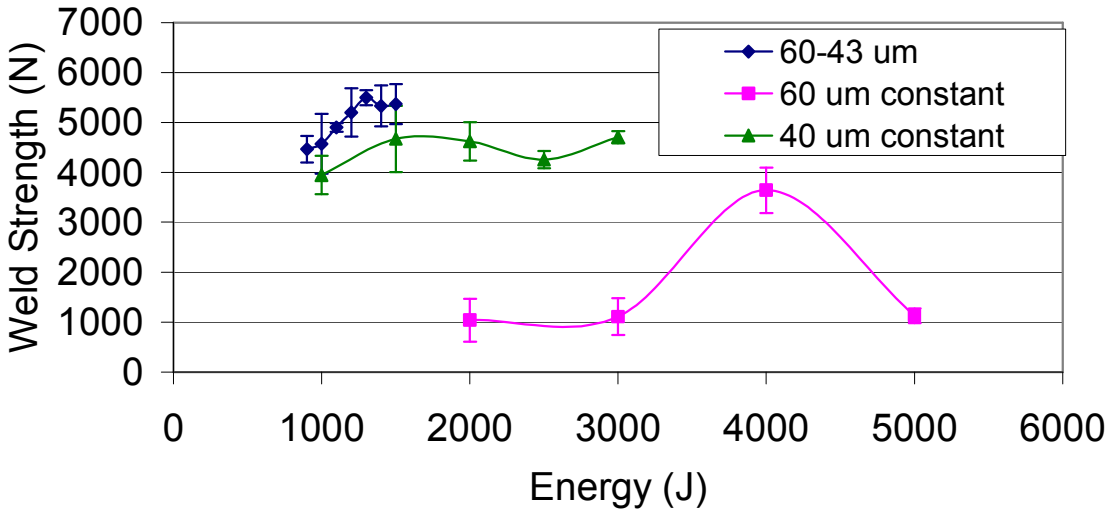

Figure 37 Weld strength with 0.1-mm Cu inserts – Strength function of energy for amplitude profiling and constant amplitude for 2-mm coupons

Due to higher weld strengths from welding with amplitude profiling, a more detailed study focused only on the amplitude profiling with and without copper buffer sheets. Figure 38 shows weld strength as a function of energy for 2-mm thick samples welded with and without 0.1-mm copper buffer sheets. The maximum weld strength achieved without copper buffer sheets was slightly over 6 kN. In comparison, the samples welded with 0.1-mm copper buffer sheets had a maximum strength of ~5.5kN. However, the copper buffer sheets reduced the part marking and the tool/part adherence. Also, it can be seen that the standard deviation is in general lower for the samples welded with 0.1-mm copper buffer sheets. It is also important to note that with the 2-mm thick sample, weld strength was not comprised noticeably by reducing part marking via copper buffer sheets.

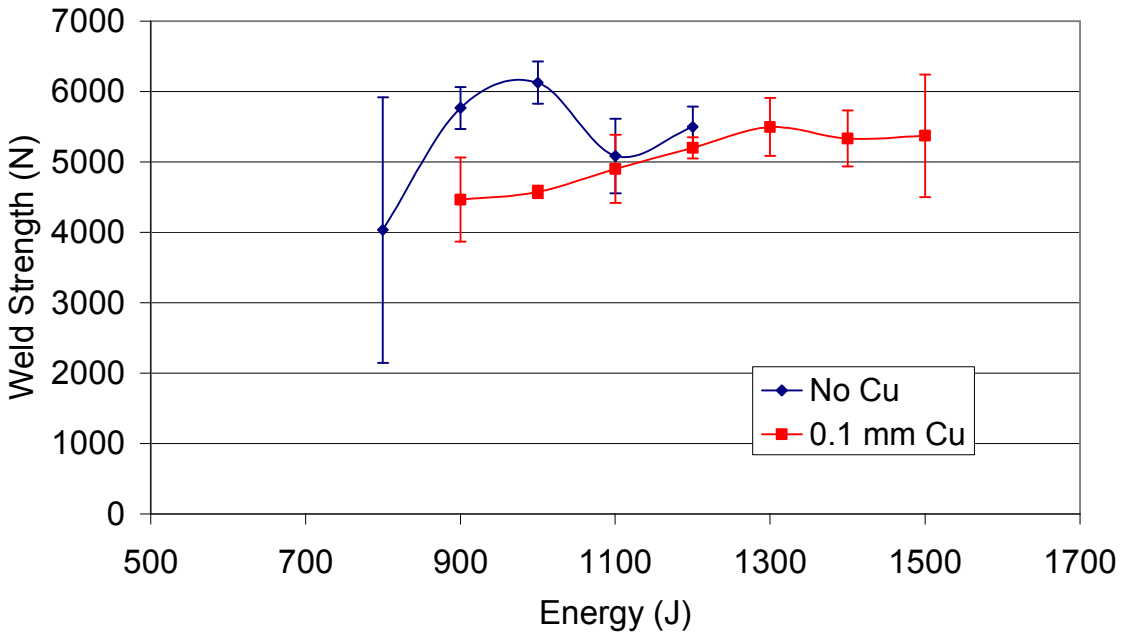

Figure 38 Weld strength vs. energy with amplitude profiling with and without 0.1-mm Cu for 2-mm samples

Figure 39 shows a photograph of part marking without the use of buffer sheets. It is seen that there is deep penetration and noticeable part marking. In addition, when disengagement of the part from the horn took place, it required relatively large force, thus part sticking was considerable.

In contrast, Figure 40 illustrates a photograph of marking of the weld made with a 0.1-mm copper buffer sheet. The sample was thick 5754 coupons and made with an energy level 3000J and an amplitude profile of 60-43 μm; despite that the welding conditions were identical, the welds made with a buffer sheet had less part marking. It is important to note that in general, even if higher energy levels are used, weld strength with buffer sheet and 3-mm-thick samples typically had lower weld strengths. For example, using the same weld energy as previously noted, when buffer sheets are used the weld strength dropped from 8000 N to 5000 N. In addition, even with higher weld energy levels, there is little increase in weld strength with buffer sheets. For the 2-mm thick samples, the drop in the weld strength was relatively minor. With the 2-mm samples the weld strength decreased from ~6000N to 5500N without and with buffer sheets respectively. It is believed that the thinner sample (2-mm) experience less attenuation and thus the buffer sheet had less adverse effects on the welding process. Thus, in final consideration for the using of buffer sheets, the importance of part marking and weld strength must be considered and balanced in how each affect the manufacturing and final product requirements. In addition the overall effect must be considered in terms of base material strength. If weld strength is critical, it is proposed to use a higher number of welds per unit length (Pitch) in order to compensate for the loss in weld strength.

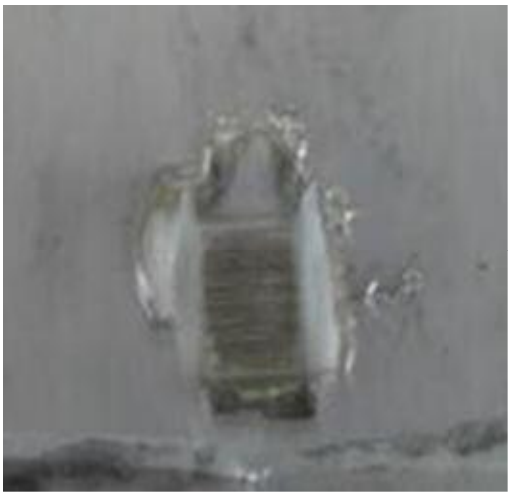

Figure 39 Without Cu buffer sheets

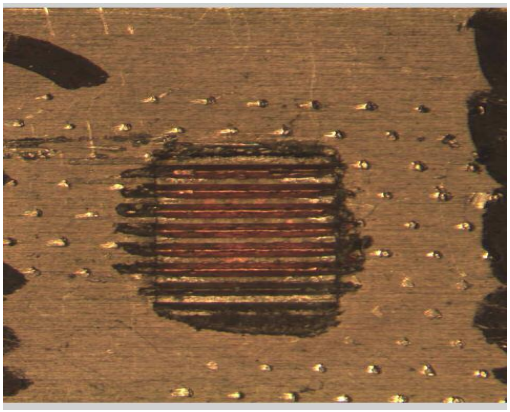

Figure 40 Photograph of part marking with 0.1-mm Cu buffer sheets

To compare the depth of penetration for the welds made with and without a copper buffer sheet, the depth was measured using a depth gauge. For example, the depth of penetration for welds made with 2-mm thick samples using 1200 J and an amplitude profile of 60-43 μm is seen in Figure 41. In this figure, it is seen that the penetration for the sample made without a buffer sheet was much larger compared to the weld made with the buffer sheet.

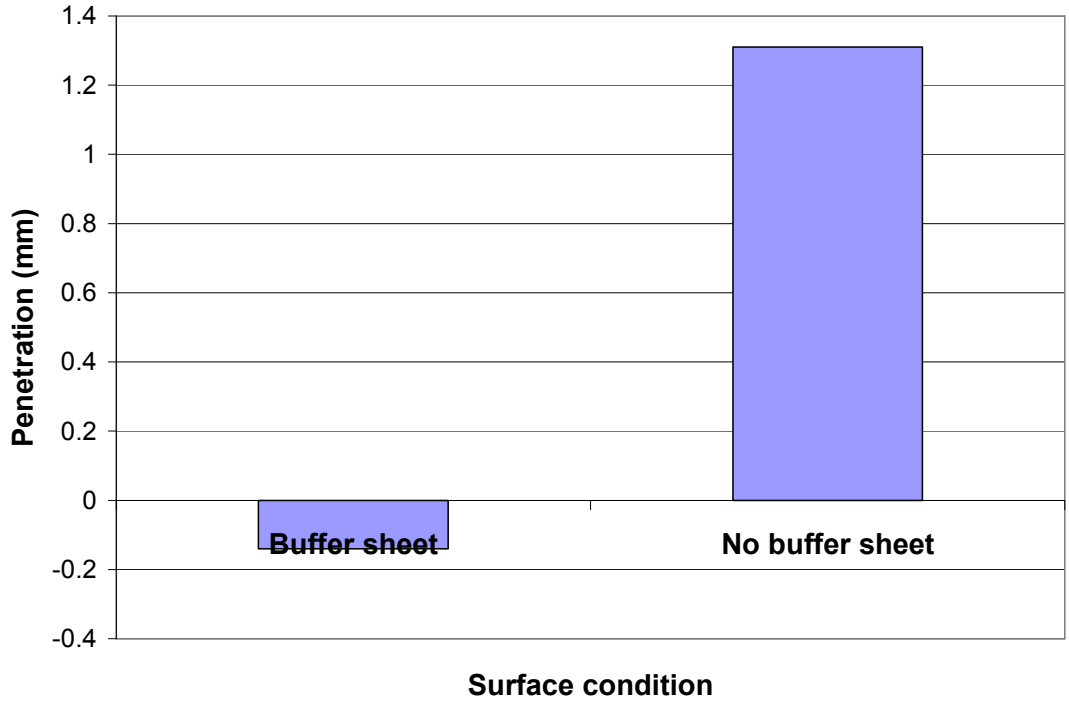

Figure 41 Penetration with and without buffer sheets (1200 J, 2-mm sample)

It is important to note that the penetration is negative for the weld made with a buffer sheet because of the displacement of material from knurled pattern on the horn. In more detail, because the penetration was nearly zero, the knurled pattern "pushed" material above the surface as depicted in Figure 42.

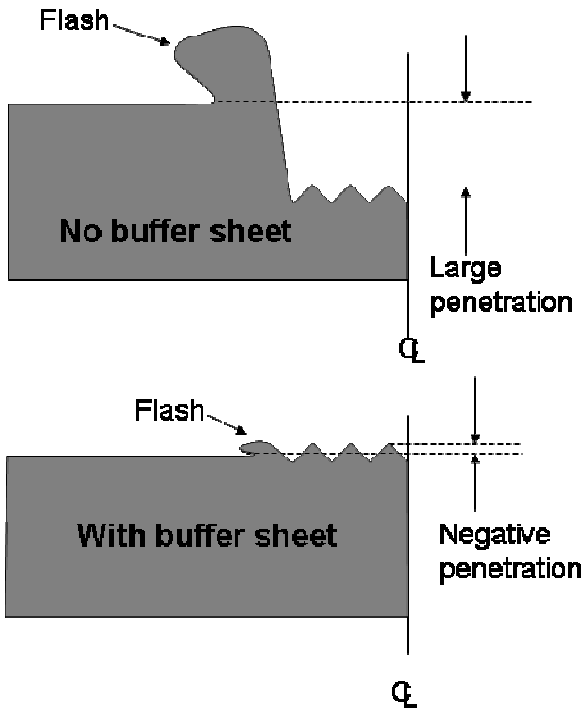

Figure 42 Cartoon detailing penetration measurements at the weld centerline (CL)

This is also seen in

Figure 43, which shows a cross section of welds made with (a) and without (b) a copper buffer sheet. As depicted in Figure 42, there is strong evidence that the amount of penetration is less when copper buffer sheets are used.

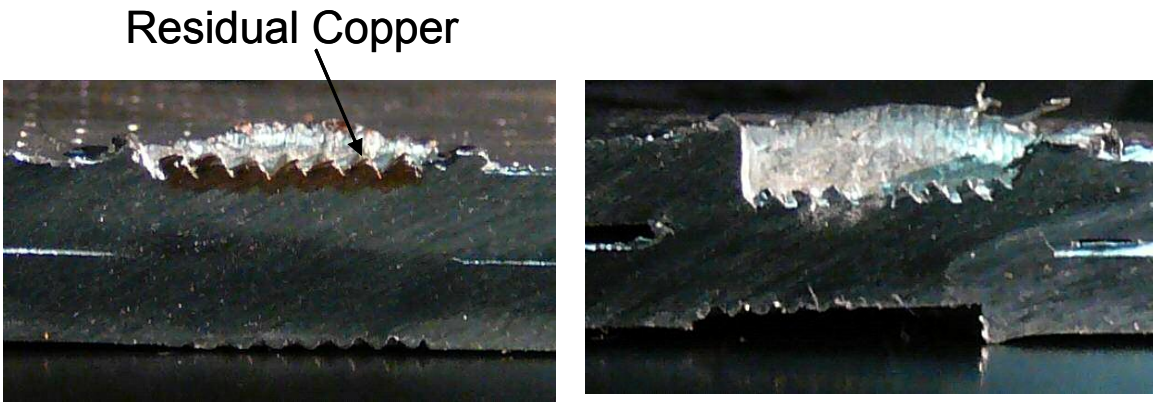

(a) (b)

Figure 43 Photograph of cross section at weld centerline of a weld made with a copper buffer sheet (a) and without (b)

Optical micrographs of the samples welded with and without 0.1-mm copper sheets

Two samples (2-mm thick samples): one welded with 0.1-mm copper sheets and the other one welded without copper sheets, were cross-sectioned, mounted, ground, polished, and etched with Kevlar's reagent in order to examine their optical micrographs.

Figure 44 shows the optical micrograph of the sample welded without copper sheets at a magnification of 5X. The weld line is relatively pronounced, being marked by the black circle.

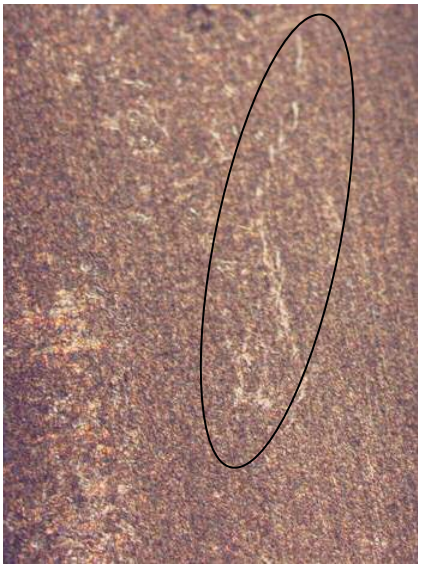

Figure 44 Optical micrograph of the weld area of the sample without copper sheet at 5X

The microstructure of the same welding at 100X is shown in Figure 45. It is seen that the weld contains large precipitates and numerous of defects. It is believed that the weld resulted in over aging of the aluminum and promoted the formation of large precipitates.

Figure 45 Optical micrograph of the welding area of the sample without copper sheet at 100X

It is important to note that the weld line of the sample welded with 0.1-mm copper sheets could not be seen at a magnification of 5X, and required a higher magnification, (10X) as shown in Figure 46. At higher magnifications the weld line remained difficult to see. The only evidence of the weld was a small a defect/crack as detailed in Figure 46.

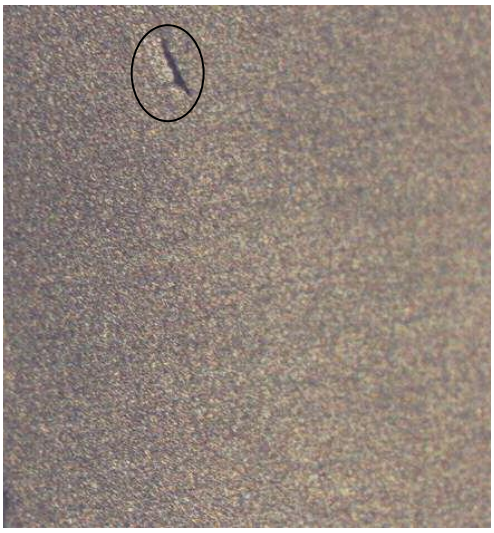

Figure 46 Optical micrograph of the weld area of the sample with 0.1-mm copper sheet at 10X

The microstructure of the same welding area for the sample welded at 100X with 0.1-mm copper is illustrated in Figure 47. It is seen that there are fewer and smaller precipitates compared to the weld made without a copper buffer sheet. This is in agreement with the theory that the buffer sheet attenuated the vibrations and reduced the heating (power) dissipated at the faying surface. This reduction in heating limits the level of over aging and growth of precipitates. It is important to note the effect over aging on the final weld strength was not noticeable and did not affect the final weld strength.

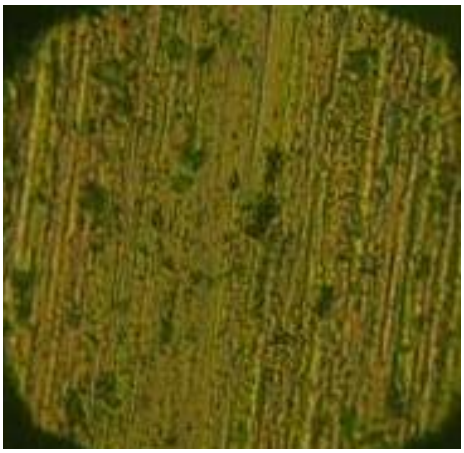

Figure 47 Optical micrograph of the welding area of the sample with 0.1-mm copper sheet at 100X

In order to gain insight into the local effects of the copper buffer sheets, additional micrographs were prepared at the part/buffer sheet interface. It was theorized that the copper and aluminum form inter-metical compounds that locally harden the sample and this reduces the part marking. That is to say, welding occurs between the copper sheet and the aluminum. The ultrasonic energy scrub the copper insert against the aluminum coupons cleaning the surface of oxides and debris exposing an oxide free surface. The welding is further enhanced by the ultrasonic energy promoting plastic deformation forcing the two metals into intimate contact. Inter-metallic diffusion of the copper and aluminum atoms occurs at the faying surface which then results in the formation of a weld. Figure 48 shows a micrograph of the inter-metallic layer formed between the copper and the aluminum alloy. The inter-metallic microstructure is of the zone directly below the horn.

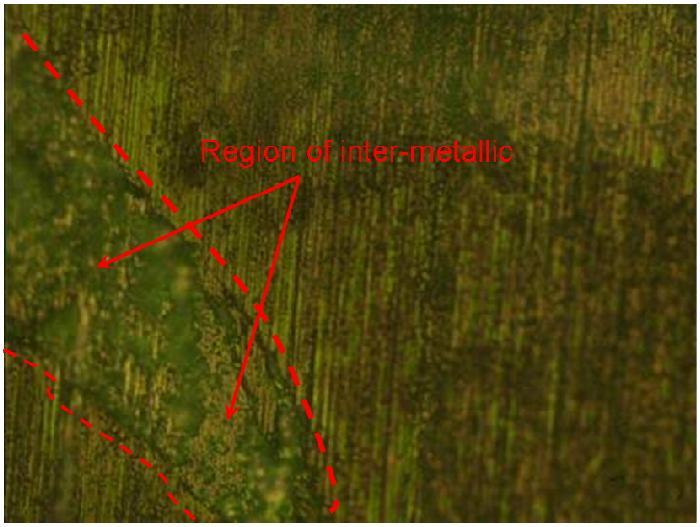

Figure 48 Optical micrographic picture of the inter-metallic layer between the Cu phase and the Al alloy, underneath the horn at 100X

The study of the coupons of aluminum 5754 using Zn buffer sheet

Figure 49 shows weld strength as a function of energy with varying thicknesses of the zinc buffer sheets. Based on the previous results that amplitude profiling promoted higher weld strength, only welds made with amplitude profiling were studied in this case. Thus, amplitude profiling of 60-43 µm was used. A number of 10 samples were welded for each energy level setting and each thickness. It is seen that the welds made with a zinc buffer sheet with a thickness of 0.125-mm produced slightly higher weld strengths. It is believed that the thicker zinc buffer sheet (0.2-mm) attenuated the ultrasonic vibrations and prevented proper welding and this accounted for the relatively week welds with this thickness. The thinner buffer sheet appeared to work nearly as well as the thicker 0.125-mm thick buffer sheet. It is important to note that only a limited number of samples were prepared with the 0.1-mm thick buffer sheet because of a limited supply of the samples. Thus, these experiments were conducted as screening experiments to confirm there was

no advantage of using thinner buffer sheets. It is important to note that the 0.125-mm thicknesses buffer sheets, greatly reduced part marking and the sticking to the horn of the coupons to be welded which is further detailed below.

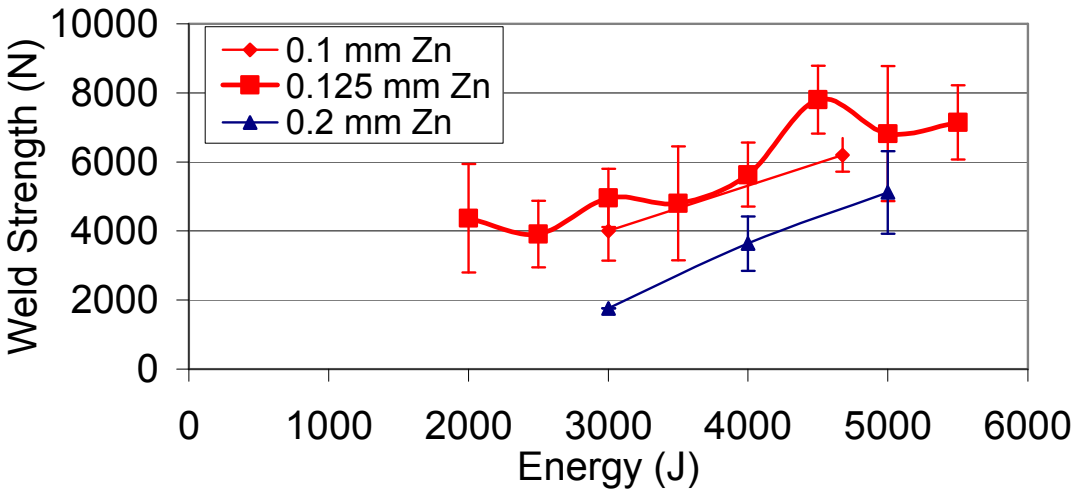

Figure 49 Strength vs. energy for amplitude profiling of 60 to 43 µm and various thicknesses of Zn inserts

Figure 50 shows a graph of the weld strength as a function of energy with 0.125-mm thick zinc buffers using a constant amplitude (60 µm and 43 µm) and amplitude profiling (60 to 43 µm). It is seen that with a constant amplitude of 60 µm or 43 µm, the weld strength is relatively low and virtually rarely exceeded 3500 N. It is believed that is due to shearing of the weld which prevented proper fusion of the faying surfaces. With amplitude profiling 43 to 60 µm, the weld strength was typically ~ 8000 N. It is important to note that with amplitude profiling and the 0.125-mm thickness of zinc buffer sheets, the part marking and the tool/part adherence were improved. Also, the cycle times for the welds made with lower amplitude were typically 2 to 3 times longer.

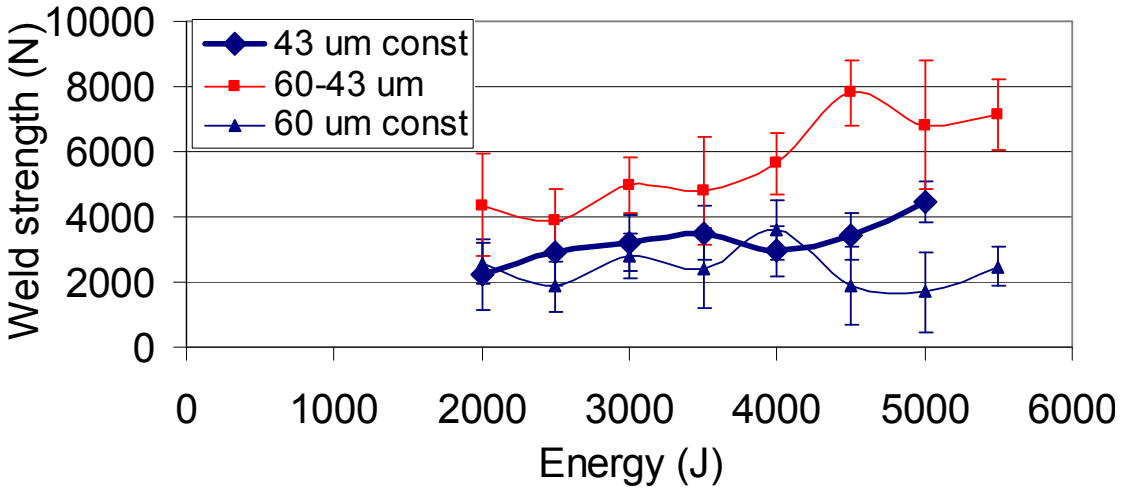

Figure 50 Strength vs. energy for amplitude profiling and constant amplitude with 0.125-mm Zn inserts

Additional experiments were with the zinc buffer sheets and amplitude profiling. For example, Figure 51 shows weld strength as a function of weld energy with and without zinc buffer (amplitude profiling only). It is seen that with the use of a zinc buffer sheet, higher value of the maximum weld strength was achieved. In addition, the part marking is also reduced as it will be detailed shortly. In more detail, welds without zinc inserts never exceeded 7000 N while in contrast, with the use of a buffer sheet the weld strength of 8000N is achievable and more importantly, the marking and sticking are reduced as can be seen from the Figure 52 (without zinc inserts) and Figure 53 (With 0.125-mm Zn) .

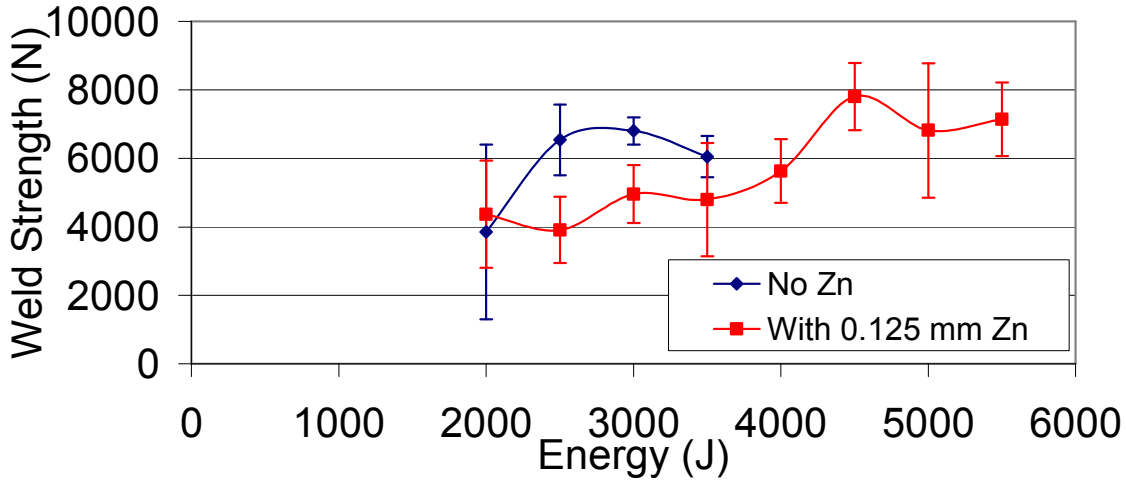

Figure 51 Weld strength function of energy -with and without 0.125-mm Zn inserts

Figure 52 Photograph of part marking without Zn buffer sheets

Figure 53 Photograph of part marking with 0.125-mm Zn buffer sheets

Optical metallography of the samples welded with and without zinc buffer sheets

Two separate samples were selected for optical metallography; one welded with 0.125-mm zinc buffer sheet and a second sample without zinc buffer sheet. They were cross-sectioned, ground, polished, and etched with various etchings in order to examine their microstructures.

Figure 54 shows the microstructure of the welding area for the sample welded without the zinc buffer sheet. It is seen that the weld contains large precipitates and numerous defects. It is believed that the weld resulted in over aging of the aluminum and promoted the formation of large precipitates. In contrast, Figure 55 shows a microstructure of the sample welded with 0.125-mm zinc buffer sheets. In this case, there is no evidence of defects or precipitates. This is in agreement that the use of zinc buffer sheets increase weld strength.

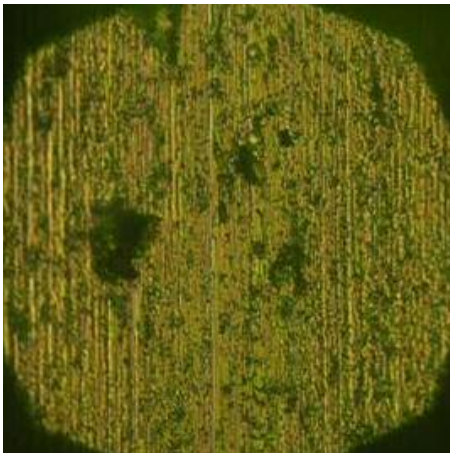

Figure 54 Optical micrograph of the weld area of a sample welded without Zn at 100X

Figure 55 Optical micrograph of the weld area of a sample welded with 0.125-mm Zn at 100X

In summary, buffers sheets reduce part marking and the sticking to the horn. The inter-metallic compounds produced by the interactions between the buffer sheets and the aluminum alloy are hard, making it difficult for the horn to penetrate into the sample.

Conclusions

Placing buffer sheets of copper or zinc between the tool (horn) and the top part prior to the ultrasonic welding of aluminum, reduced the tool/part adhesion and part marking. Also, the use of zinc buffer sheets (0.125-mm thickness) during the ultrasonic welding of aluminum 5754 alloy resulted in higher maximum weld strength values compared to using the copper buffer sheets (0.1-mm thickness). It was seen that copper buffer sheets reduced weld strength and this effect is more pronounced with thicker (3-mm) weld samples.

It was also seen that the thickness of the buffer sheets should be reduced to 0.1 to 0.125-mm in order to prevent attenuation of the energy.

The micrographs of the welded samples with copper sheets showed large and numerous precipitates distributed near the weld zone. In contrast, the samples welded with zinc buffer sheet had a microstructure characterized by a very fine and uniform morphology, resulting in higher weld strength.

Thus in summary:

- Buffer sheets significantly reduced part marking and part/tool adhesion
- Zinc buffer sheets resulted in higher weld strength compared to copper buffer sheets
- Copper buffer sheets reduced weld strength especially for thick samples
- Samples welded with zinc- very fine and uniform morphology–higher weld strength
- Samples welded with copper –large and numerous precipitates–lower weld strength

References

1. Beyer, W., "The bonding process in the ultrasonic welding of metals", Schweisstechnik, Jan. 1969, v.19, n. 1, pp. 16-20.
2. Totten, G., MacKenzie, S., *Handbook of aluminum-Alloy Production and Materials Manufacturing,* Vol. 2. 2003
3. Davis, J. R., Davis & Associates, *Aluminum and Aluminum Alloys,* ASM Specialty Handbook, 1993
4. Dossert, Technical information, *Corrosion and Connectors,* http://www.dossert.com/technicalinfo/corrosion.htm

CHAPTER 4: COMPARISON OF CONTROL ALGORITHMS FOR ULTRASONIC WELDING OF ALUMINUM

To be submitted to American Welding Society Journal

Maria Vlad, David Grewell

Abstract

Although ultrasonic metal welding is energy and time efficient, there have been problems related to weld consistency when using energy as a control mode. To resolve these issues, a comparison between three control modes: energy, height (post height), and time was conducted and the results were analyzed. Thus, the main objective of this study was to characterize the weld consistencies of the various control modes. The control mode resulting in maximum weld strength values and consistent welds was considered the optimum one. In this study, 60 welds made with optimum welding parameters with each mode were done and the average weld strength and variance of the population were statistically compared. It was determined by analyzing the data with an F-test with a probability α=0.05 that there was a slight improvement in weld strength consistency for the time mode compared to the other two modes (energy and post height).

In addition, no significant difference in the average weld strength was seen for the three modes.

Introduction and background

Ultrasonic metal welding invented over 50 years ago is a process that consists of joining two metals by applying ultrasonic vibrations under moderate pressure. The high

frequency vibrations locally soften the overlap zone between the parts to be welded forming a solid-state weld through progressive shearing and plastic deformation. The oxides and contaminants are removed by the high frequency motion ("scrubbing") producing a pure metal/metal contact between the parts allowing the intermetallic bonds to take place. Beyer states that "Ultrasonic welding of metals consist of interrelated, complex processes such as plastic deformation, work hardening, breaking of contaminant films, fatigue crack formation and propagation, fracture, generation of heat by friction and plastic deformation, re-crystallization, and interdiffusion." [1] Also, it is worth mentioning that "The dominating mechanism for ultrasonic welding is solid state bonding, and it is accomplished by two different processes: Slip and plastic deformation."

During welding, the machine control is usually set to a particular mode. For example, for the energy mode, the power supply will monitor the power and integrate the value over time. Once a present amount of energy is dissipated, the power supply discontinues the ultrasonic energy, independent of the time. In contrast, in the time mode the sonics remain on for a present length of time, independent of the energy. In the last mode, post height, the power supply monitors an encoder on the actuator and continue to apply ultrasonic energy to the parts until the preset amount of displacement occurs. The post height is defined as the gap between the final position of the horn and anvil as seen in Figure 56.

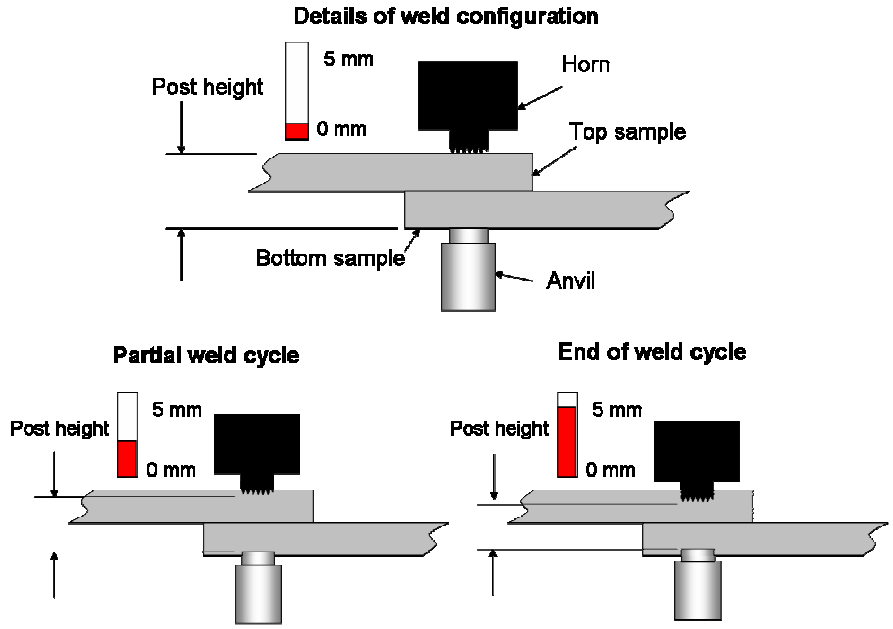

Figure 56 Illustration of the postheight measurement

It is important to note that it is industry standard to use an energy mode for process control and post height is a relatively new technology for the industry.

Objective

Thus, the main objective of this study was to characterize the weld consistencies of the various control modes. Because weld strength variation is a major issue related to ultrasonic metal welding, determining which control parameters could increase weld consistency would reduce waste and improve productivity in industry.

Experimental procedure

Experimental design

To determine the optimum welding conditions for the various modes: energy, post height, and time, the energy mode was initially studied because it represents the mode most commonly used in industry. A total of 10 samples were welded with each energy level varying from 2000J to 5500J with increments of 500J, in increasing order, not randomized. The energy value that resulted in the highest weld strength while using the energy control mode was selected as the optimum weld energy. The corresponding average weld time (1.0s) and average post height (4.6 mm) from this optimum weld energy value, were used as initial welding parameters for the other modes (time and post height). For example, in order to identify the optimum time and post height values, additional welds were made with a range in times between 0.6s to 2s and range in post height between 4.3-mm to 5 mm. For each condition, 10 welds were made and tested. Based on these results, the optimum welding parameters for each mode was selected and 60 welds were made with each mode for a total of 180 welds.

To compare the weld consistency between the various modes a statistical F-test was used. In order to replicate industry practice, the welds were not randomized.

Weld amplitudes that were studied ranged from 40 to 60 μm_{pp}. Additional details of the amplitude settings are defined in the *equipment* section. The weld force was set to a constant value of approximately 3400 N.

Materials

The ultrasonic metal welding was completed with aluminum 5754 coupons of two different thicknesses: 2-mm and 3-mm. The 5754 aluminum alloy was used in an as received condition, in the O-temper condition. Large sheets (~30 cm x 30 cm) sheets were provided by Ford Motor Company and the sheet sheared to produce 25.4 mm x 100 mm samples (1" x 4" in). The typical chemical composition for the 5754 aluminum alloy is: 2.6-3.2% Mg, 0.5% Mn, 0.4% Fe, 0.4% Si, the balance being aluminum. The weld sample configuration was a 25.4 mm x 100 mm and the weld configuration will be 25.4 mm (1 in) in overlap with the weld at the center of the overlap.

Equipment

The weld amplitude was varied using a WPC-1controller manufactured by Branson Ultrasonic Corp. The controller has the ability to vary the amplitude profiling at two separate values (A and B) with various switch over modes. The switch over mode is the parameter that defines when the amplitude is switch from value A (typically 60 μm_{pp}) to B (typically 43 μm_{pp}). For example, the mode can be set to time, energy and peak power. In this work only time was evaluated as this is the simplest mode to visualize and decouple from other welding parameters. In screening experiments, different amplitudes (50 and 58 μm_{pp}) were also studied, but the resulting weld strength and consistency was lower (~3000N) than the ones described in this paper. Welds were made at various energy levels, where the energy level was calculated by the power supply. In this case the power supply digitally integrated the power curve and the sonics remained active until a preset level of energy was dissipated. The typical range of pre-set energy levels

was between 500 and 5500 J, depending on the weld quality and the equipment capacity. For example, if the energy level was too low, the weld was not complete, and if the energy level was too high, part marking was excessive and equipment could overload. This range was selected based on screening experiments and experience.

The welding system was manufactured by Branson Ultrasonic Corp. The horn was a standard knurled tip as shown in Figure 57. The anvil was a standard “flex” anvil also detailed in Figure 58. The weld force was held constant at 3360 N (750 lbs). A squeeze time of 0.2 seconds was used to allow the force to fully develop prior to activation of the sonics. The actuator was a specially designed pneumatic linear system that had linear rail to reduce rotation of the stack assembly during welding.

Figure 57 Picture of the horn

Figure 58 Picture of the anvil tip and knurl pattern

Characterization

All welds (10 samples for every energy level) were tested in tension at a cross head speed of 10 mm/min. The maximum sustained load was used to calculate the ultimate strength. The testing method is shown in Figure 59. It is seen that shims were not used in the grips with the sample and thus bending stresses were not minimized.

Figure 59 Picture of the testing weld strength

Results and discussion

Energy Mode Optimization

Using the energy control mode, Figure 60 shows weld strength as a function of energy with constant amplitude and amplitude profile. There are several trends that can be seen in this graph. For example, the welds made with amplitude profiling of 60 to 43 µm had a relatively lower range of variation of the weld strength compared to those welds made with constant amplitude of 43 µm. The maximum weld strength for the welds made with amplitude profiling was approximately ~8 kN while in contrast the maximum weld strength made with a constant amplitude was only approximately 5.5 kN. Again, the weld cycle time was reduced when amplitude profiling was used. The average time was 1.1 s and the average post height was 4.6 mm.

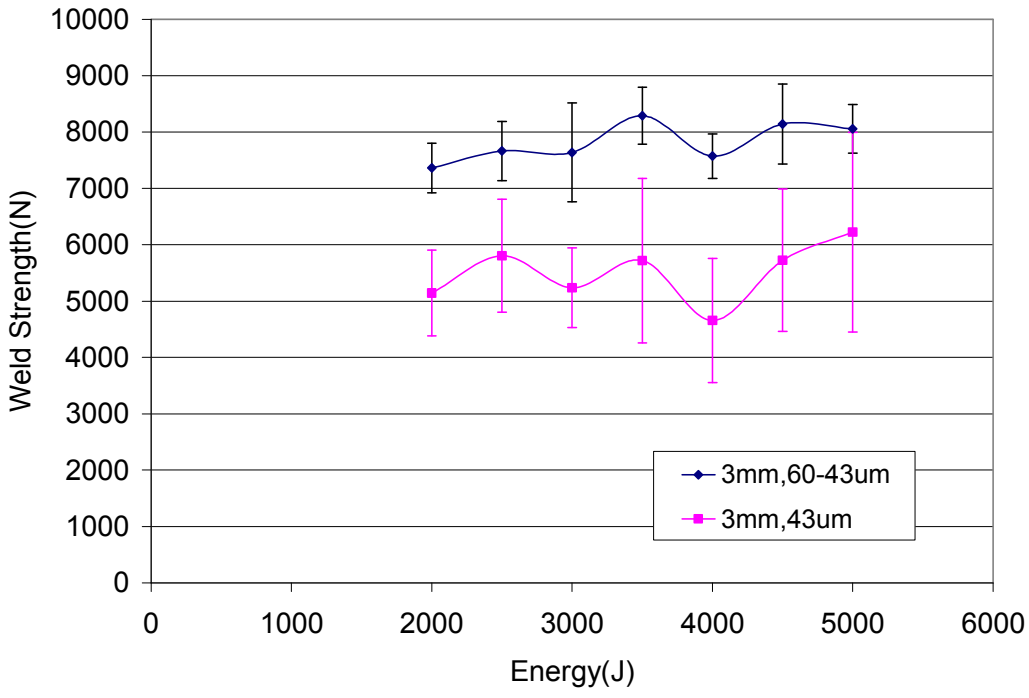

Figure 60 Strength vs. energy for amplitude profiling and constant amplitude

Post Height mode optimization

Based on previous results, welds were made in the post height mode at various post height setting using constant and profiled amplitude. As seen in Figure 61 (weld strength as a function of post height), welds made with amplitude profiling, again appear to be stronger. It is important to note that a constant higher amplitude (60 µm) was not included in this study because as previously detailed in Chapter 3, a constant higher amplitude promote shearing of the weld and reduces weld strength.

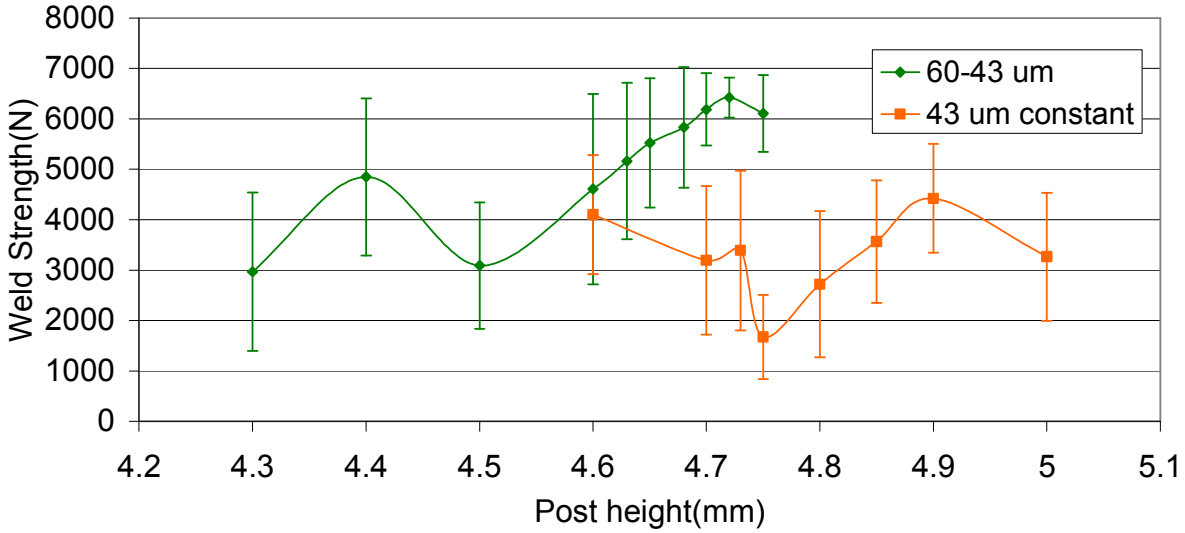

Figure 61 Weld strength as a function of postheight values using a constant amplitude and amplitude profiling

Again referring to Figure 61 by using amplitude profiling (60 to 43 µm) the optimum post height value was selected as 4.7 mm which produced a maximum weld strength over 6500 N. In contrast welds made with a constant amplitude produced a maximum weld strength value of only 4.5 kN at a post height of 4.9 mm.

In order to gain insight into the welding process, two samples, one at the optimum welding post height (4.7 mm) and one at the minimum welding post height (4.3-mm),

were selected for optical-microscopy. One sample from each population was cross-section cut, mounted, ground, polished and etched.

Figure 62 shows the micrographs of the sample welded with a post height of 4.3-mm (over welded sample). It is seen that the interface (faying surface) has multiple crack and defects between the coupons caused by a relatively large amount of penetration beyond the optimum conditions.

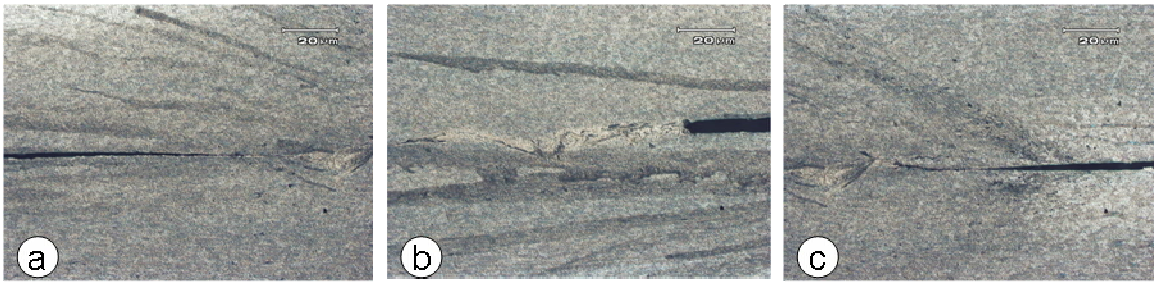

Figure 62 50X micrographs of the welding area of the sample welded with a postheight of 4.3-mm (a) left edge of weld (b) center of weld and (c) right edge of weld

Figure 63 shows a higher magnification at the interface for the sample welded with a post height of 4.3-mm. It is further seen, there are large voids and cracks (emphasized by the blue ovals) and evidence of fracture of the faying surfaces. It is believed that this weld fracture is due to over welding and shearing of weld even though amplitude profiling was used. This results in a non-uniform microstructure and therefore a relatively low weld strength sample.

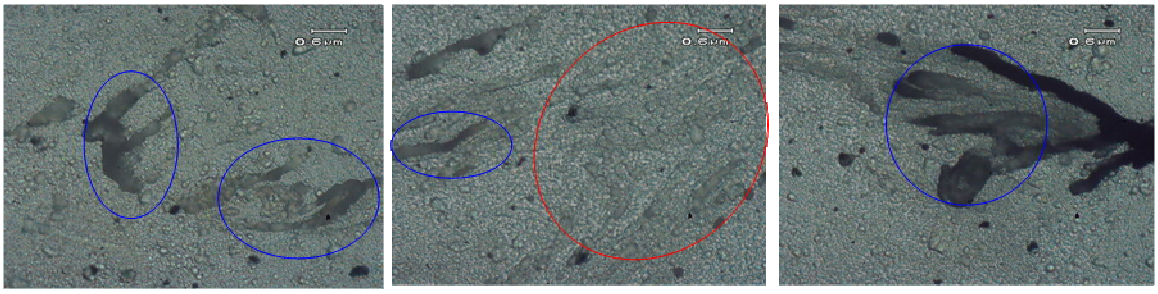

Figure 63 1000X micrographs of the welding area of the sample welded with a postheight of 4.3-mm

Figure 64 shows the micrographs of the sample welded with post height of 4.75 mm (optimum welding parameter). In this case, more fusion is seen at the faying surface as evident of no cracks as well as a nearly invisible weld line.

Figure 64 50X micrographs of the welding area of the sample welded with a postheight of 4.75 mm (a) left edge of weld (b) center of weld and (c) right edge of weld

Figure 65 shows a micrograph of the interface of the welding zone for the sample welded with a post height of 4.75 mm at a magnification of 1000x. Again it is seen that the microstructure is more uniform with little evidence of pores/voids compared to the

microstructure of the weld made with a post height value of 4.3-mm. The fusion appears to be more pronounced being emphasized in the red oval.

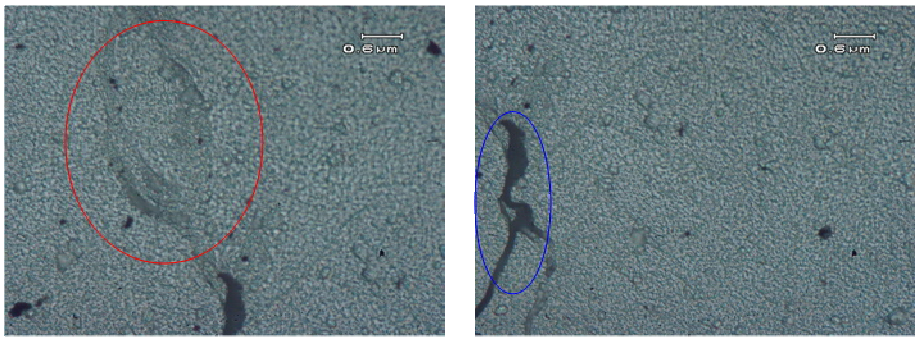

Figure 65 1000X micrographs of the welding area of the sample welded with a postheight of 4.75 mm

Time mode optimization

Figure 66 shows weld strength as a function of weld time with and without amplitude profiling. Again, a constant amplitude at the higher level (60 μm) was excluded from this study because it has already been shown to produce relatively low weld strengths. Again it is seen that amplitude profiling produced relatively higher weld strengths, compared to constant amplitude.

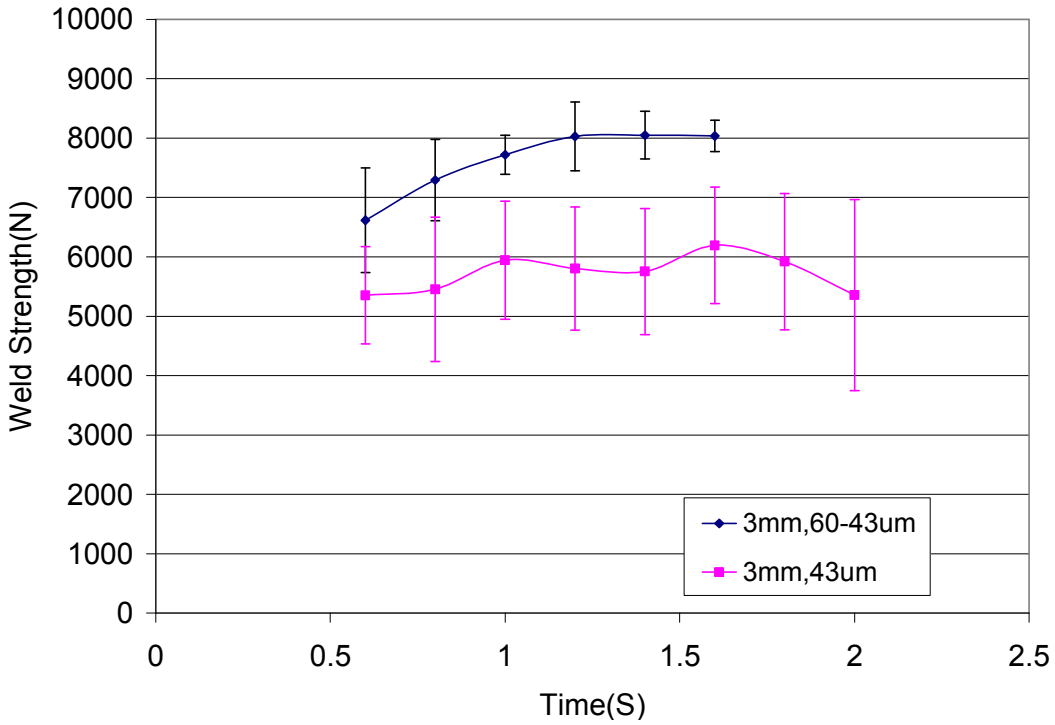

Figure 66 Graph of the weld strength function of the preset time values using constant amplitude and amplitude profiling

Figure 66 suggests that by using amplitude profiling, the standard deviation is relatively low over the time range studied compared to the standard deviation of the constant amplitude case. It is important to note that in this study, the population size was 10 and thus, thus this is only a general observation. The optimum weld strength when using the amplitude profiling was ~8 kN with a weld time of 1.2 s and the optimum weld strength value for the constant amplitude was ~6 kN reached with a weld time of 1.7 s.

Statistical Comparison

In comparing the three control algorithms, it is important to note that the average weld strengths for all: energy, post height, and time were very similar and fell within the standard deviations of each other, as seen in the Figure 63. In more detail, this graph

shows the average weld strength (bar height) for the 60 welds made with each mode and the standard deviation is detailed by the corresponding error bars. The over all average for all three modes (180 welds) is highlight with the black horizontal line. It is seen that the average strength for the modes are very similar to each other and all fall within each other standard deviation. In order to confirm that the average weld strengths were not significantly different a standard t-test was conducted. Table 5 details the results of the test comparing the t-test values for the average weld strengths comparing the three modes. For example, in comparing the energy and post height modes, the t-test value is 0.2405 which corresponds to a 66% (100%-24.05%) confidence level that there is a difference between the two average values. Because this confidence level is relatively low, there is no significant evidence that there is a difference between the two modes: energy and post height. In addition, when comparing the other modes: post height with time and energy with time, it is seen that the t-test values are higher, 0.6587 and 0.4631 respectively, thus the confidence level that there is any difference between any of these two populations is even lower. Thus, it is proven that there is no significant difference between the average weld strengths of any of the three populations.

Table 2 Statistical t-test values for the average weld strengths for the 3 controls modes

Mode/Mode	**Energy**	**Post Height**	**Time**
Energy	N/A	0.2405	0.4631
Post height	0.2405	N/A	0.6587
Time	0.4631	0.6587	N/A

In addition, there is no strong indication that any one particular mode is more consistent in that the standard deviations are similar, with the time mode having a slightly smaller deviation compared to the other control modes.

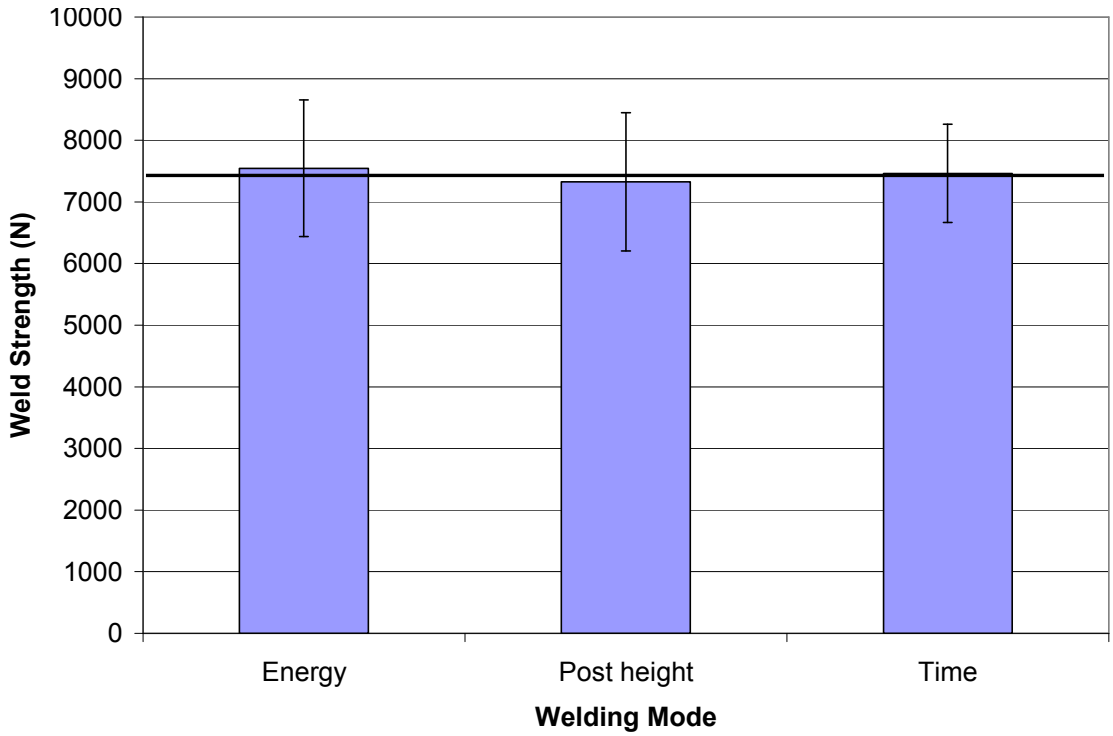

Figure 67 Bar graph of the average weld strengths of the three modes: energy, post height, time

As previously noted, in order to further compare weld strength variance, Table 3 shows the statistical analysis of the data for the comparison between the post height and energy mode. The energy mode was considered the baseline mode as it is the mode most commonly used by industry [2]. This analysis is intended to prove whether the difference in the variance of the two populations (energy, post height) is significant. This approach is commonly used when the standard deviation of two populations is being compared. It is important to note that the population size was 60 for each control mode. For such a sample size (i.e., 60), if F>2.354 then it is possible to state that it has been proven with alpha = 0.05 and β=0.05 that there is a significant difference between the variances of the two populations compared.

For example, as seen in Table 3 the post height mode variance (1259047) compared to the energy mode variance (1228052) has an F_{calc} value of 1.025, thus because F_{calc} <1.54 there is no significant difference between the two modes in terms of variance.

Table 3: Statistical analysis of the comparison between energy and post height mode

	Energy	***Post height***
Mean (N)	7546	7327
Variance	1228052	1259047
Observations	60	60
Df	59	59
F	0.975	**1.025**
P(F<=f) one-tail	0.462	
F Critical one-tail	0.649	**1.54**

Table 4 details the statistical analysis of the data for the comparison between the energy and time mode. The energy mode variance (1228052) versus the time mode

variance (636453) has an F_{calc} value of 1.930. Because F_{calc} =1.54 <1.93 there is a significant difference between the variances of the two populations compared: energy and time.

Table 4: Statistical analysis of the comparison between energy and time modes

	Energy	***Time***
Mean (N)	7546	7464
Variance	1228052	636453
Observations	60	60
df	59	59
F	**1.930**	
P(F<=f) one-tail	0.006	
F Critical one-tail	**1.540**	

Table 5 details the statistical data of the comparison between the post height and time mode. The post height mode variance (1259047) versus time mode variance (636453) has an F_{calc} value of 1.978, thus because F_{calc} =1.54<1.98, there is a significant difference between the two populations compared: post height and time.

Table 5: Statistical analysis of the comparison between post height and time modes

	Post height	***Time***
Mean (N)	7327	7464
Variance	1259047	636453
Observations	60	60
df	59	59
F	**1.978**	
P(F<=f) one-tail	0.005	
F Critical one-tail	**1.540**	

Therefore, for a population size of 60, the time mode resulted in weld strength values that were more consistent. That is to say, the weld strength variance for those welds made with the time mode was smaller than that for the welds made in the height and energy mode.

Conclusion

In this study it was statistically proven that the weld strength variance for those welds made with the time mode was smaller than that for the welds made in the height and energy mode. In addition, when each mode is optimized, they produced comparable average weld strength. In addition, it was seen that over welding in post height mode resulted in large voids at the faying surface.

Thus in summary:

- The weld strength variance for the time mode smaller compared to the other two modes
- When each mode is optimized – produce comparable average weld strength
- The micrographs showed that over welding in post height mode resulted in large voids at the faying surface

References

1. Beyer, W., “The bonding process in the ultrasonic welding of metals”, Schweisstechnik, Jan. 1969, v.19, n. 1, pp. 16-20.
2. Grewell, D., Gneiting, R., Strohm, G., Benatar, A., *Comparison of Control Algorithms for Ultrasonic Welding of Plastics,* Ohio State University.

CHAPTER 5: GENERAL CONCLUSIONS

In this study it was seen that over simplified models reasonably predicted the dissipated power during ultrasonic metal welding. Measured power levels were in the range of 2000 to 3000 W and the models, based on friction and velocity, predicted power levels in the range of 3000W. In addition, a simple one-dimensional heat flow solution accurately predicted bondline temperature for the initial phase of the weld. However, after softening of the sample, the model over predicted the temperature. It was also seen in this study that amplitude profiling allows better matching of amplitude to the various phases of the weld. For example, by initiating the weld with relatively high amplitude, fast and efficient welding is promoted. Once the material is softened, the amplitude can be reduced to minimize shearing of the weld. Thus, amplitude profiling increases weld strength and reduces weld time. However, the amplitude profiling did not affect the tool/part adhesion, thus there was no improvement of the horn adhesion to the top part during welding.

Placing buffer sheets of copper or zinc between the tool (horn) and the top part prior to the ultrasonic welding of aluminum reduced the tool/part adhesion and part marking. Also, the use of zinc buffer sheets (0.125-mm thickness) during the ultrasonic welding of aluminum 5754 alloy resulted in higher weld strength values compared to using copper buffer sheets (0.1-mm thickness). It was seen that copper buffer sheets reduced weld strength and this effect is more pronounced with thicker (3-mm) weld samples.

It was also seen that the thickness of the buffer sheets should be minimized to 0.1 to 0.125-mm in order to prevent attenuation of the energy.

The micrographs of the sample welded with copper sheets showed precipitates generated by over aging of the samples. In contrast, samples welded with zinc buffer sheet had a microstructure characterized by fine and uniform morphology, resulting in higher weld strength.

It was statistically proven that the weld strength variance for those welds made with the time mode was smaller than that for the welds made in the height and energy mode. In addition, when each mode is optimized, they produced comparable average weld strength. In addition, it was seen that over welding in post height mode resulted in large voids at the faying surface.

Future work

Future research should include welding of larger samples and actual automotive applications. Work should also evaluate the alternative tooling design, buffer sheet composition, tip coatings and the isolation of vibrations. The coupling of various control modes should also be evaluated to determine if any of the modes can be synergetic to increase weld consistency.

REFERENCES

1. Totten, G., MacKenzie, S., *Handbook of aluminum-Alloy Production and Materials Manufacturing,* Vol. 2. 2003
2. Davis, J. R., Davis & Associates, *Aluminum and Aluminum Alloys,* ASM Specialty Handbook, 1993
3. The Institute of Materials, Minerals and Mining. *Materials World*. Vol. 12 **(3)**. 37-38. March 2004
4. Kelkar, A., Roth, R., Clark, J., *Automobile bodies: Can Aluminum be an economical alternative to steel,* Automotive Materials: Economics, Journal JOM, Vol. 53 **(8)**, 2001, pp. 28-32.
5. European Aluminum Association, *Aluminum in the automotive industry,* 1996.
6. Aluminum Association, *Sorting the wrought from the cast in automotive aluminum*, 2003.
7. Wikipedia-The Free Encyclopedia, *Gas Tungsten Arc Welding,* *http://en.wikipedia.org/wiki/Gas_tungsten_arc_welding*
8. Introduction and chapter objectives, http://www.kunststoffweb.de/bookshop/pdfs/45614lp.pdf
9. Joshi, K., *The Formation of Ultrasonic Bonds between Metals*, Welding Journal, December 1971, No.12, pp. 840-848.
10. Beyer, W., *The bonding process in the ultrasonic welding of metals*, Schweisstechnik, Jan. 1969, v.19, n. 1, pp. 16-20.

11. Hazlett, T., Ambekar, S., *Additional Studies on Interface temperatures and bonding mechanism of Ultrasonic welds*, Welding Journal, May 1970, pp. 196-200.

12. Pfluger, A., Sideris, X., *New developments in Ultrasonic Welding*, Sampe Quarterly, Oct. 1975, v. 7, n. 1, pp. 9-19.

13. Wodara, J., *Joint formation in the Ultrasonic welding of Metallic Substances*, ZISMitteilungen, 1986, v.28, n. 1, pp. 102-108.

14. Garcia, J. A., Mandelis, A., Farahbakhsh, B., Lebowitz, C., Harris, I., *Thermophysical Properties of Thermal Sprayed Coating on Carbon Steel Substrates by Photothermal Radiometry*, Int. J. of Thermophys**,** 1999, Vol. 20 (5), 1587-1602.

15. The Engineering Tool Box, 2005, http://www.engineeringtoolbox.com/specific-heat-metals-d_152.html

16. United States Steel Corporation, 2005. http://www.ussautomotive.com/auto/steelvsal/hood.htm

17. de Vries, E., *Mechanics and Mechanisms of Ultrasonic Metal Welding*, *Dissertation,* Ohio State University, 2004.

18. Grewell, D., *Study on amplitude droop*, Branson Co.

19. Stokes, V.K., *Vibration welding of Thermoplastics*. Part I, *Polymer Engineering and Science*, June, 88, Vol. 28, No. 11, Society of Plastics Engineers, Brookfield, CT.

20. Rohsenow, W.M., Choi, H., *Heat, Mass, and Momentum Transfer* (1961) Prentice-Hall, Englewood Cliffs, N.J

21. Gutensohn, M., Wagner, G., Eifler, D., *Reduction of the Adherence of Aluminum on Ultrasonic Welding Tools,* University of Kaiserslautern

VITA

May 16, 1976……Born, Slatina, Olt, Romania

1999……..B.S., Department of Materials Science and Engineering, Polytechnic Institute, Bucharest, Romania

2000..……M.S., Department of Materials Science and Engineering, Polytechnic Institute, Bucharest, Romania

2005……..M.S., Industrial Technology, Iowa State University, Ames, IA, USA

2005 to present…….Assistant Scientist I, Industrial and Agricultural Technology, Department of Agricultural and Biosystems Engineering, Ames, IA USA

2006 to present……PhD student, Industrial and Agricultural Technology, Department of Agricultural and Biosystems Engineering, Ames, IA USA

PUBLICATIONS

1. Vlad M., Srinivasan G., Grewell D. (2007), *Improvement of the mechanical properties of soy protein based plastics,* ***65th Annual Technical Conference for the Society of Plastic Engineers Proceedings, Society*** of Plastics Engineering, Cincinnati, OH.

2. Vlad M., Harmon G., Grewell D., Benatar A. (2006), *Weldability of Bio-Renewable Ultrasonic Exfoliated Nanocomposites*, ***64th Annual Technical Conference for the Society of Plastic Engineers Proceedings***, Society of Plastics Engineering, Brookfield, CT

3. Vlad M., Jane J., Mungara P., Grewell D. (2006), *Mechanical properties of soy protein isolate/soy hydrolysate plastics*, ***64th Annual Technical Conference for the Society of Plastic Engineers Proceedings,*** Society of Plastics Engineering, Brookfield, CT.

4. Vlad M., Jane J., Mungara P., Grewell D. (2005), *Mechanical properties of soy protein isolate/soy hydrolysate plastics*, ***Global Plastics and Environmental Conference***, Society of Plastics Engineering, Atlanta, GA.